

California Leaking Underground Fuel Tank (LUFT) Historical Case Analyses

Authors

**David W. Rice
Randolph D. Grose*
Joel C. Michaelson**
Brendan P. Dooher***
Donald H. MacQueen
Stephen J. Cullen**
William E. Kastenberg****
Lorne G. Everett**
Miguel A. Marino***

**Submitted to the California State Water Resources Control Board
Underground Storage Tank Program and the
Senate Bill 1764 Leaking Underground Fuel Tank Advisory Committee**

November 16, 1995

*** University of California, Davis
** University of California, Santa Barbara
*** University of California, Los Angeles
**** University of California, Berkeley**

**Environmental Protection Department
Environmental Restoration Division**

Acknowledgments

Funding for this work was provided, in part, by the U. S. Environmental Protection Agency through the California State Water Resources Control Board, Underground Storage Tank Program. As UST Program Manager, James Giannopoulos, provided the wisdom and fortitude to undertake a data gathering and analysis effort of this magnitude.

A number of dedicated individuals have contributed to the research and preparation of this report. The University of California LUFT Team wishes to recognize Kevin Graves, San Francisco Regional Water Quality Control Board, for his leadership and creativity as father of the "Plumathon", as this project was known to its researchers. The UC Team also wishes to recognize Rick Rempel, Kaye McGee, and Heidi Temko, State Water Resources Control Board, who contributed ideas and skill during all phases of this project. In addition, the "hunter-gatherer" team that spent many long hours on the road copying and transcribing data from original case files must be recognized. This effort was critical to the success of this project. Finally, the authors would like to thank the following individuals for their dedication, expertise, and hard work that made this project successful.

S. Clister

R. Depue

D. Gresho

C. Kuks

N. Prentice

R. Ragaini

D. Schmidt

J. Yow

Contents

Executive Summary	EX-1
1. Introduction.....	1
1.1 Historical LUFT Case Analysis Goals	1
2. Methods	2
2.1 Historical LUFT Case Data Collection.....	2
2.2 Data Analysis Procedures	3
2.3 Estimated Hydrogeologic Parameters.....	4
2.4 Groundwater Gradient Calculations	4
2.5 Evaluation of Spatial Distribution of Hydrogeologic Parameters Affecting FHC Fate and Transport	5
2.6 Plume Length Estimations	6
2.7 Temporal Analysis of Benzene Plume Average Concentration and Length	7
3. Results.....	7
3.1 Groundwater Chemistry.....	7
3.2 Hydrogeologic Characteristics	8
3.3 LUFT Plume Characteristics	9
3.4 Temporal Changes in Average Benzene Concentration and Plume Length.....	9
3.5 Impacts of Remediation on Plume Length and Average Benzene Concentration	11
4. Discussion.....	14
4.1 Do FHC Plumes Behave in Predictable Ways?	14
4.2 What Factors Influence the Length and Mass of FHC Plumes?.....	15
4.3 To What Extent Are FHC Plumes Impacting California's Groundwater Resources?	17
4.4 How Are Data Used in LUFT Decision-Making Approach?	17
4.5 Other Needed Data	18
Appendix A	A-1
Appendix B	B-1
Appendix C	C-1

Appendix D	D-1
Appendix E	E-1
References	R-1
Acronyms	

Executive Summary

This historical leaking underground fuel tank (LUFT) case study report is submitted to the State Water Resources Control Board (SWRCB) Underground Storage Tank (UST) Program and the California Senate Bill 1764 LUFT Advisory Committee.

The primary historical LUFT case study goal is to support revision of the LUFT corrective-action process. LUFT case historical data have been collected for about ten years. Analysis of this data can provide information about the fate and transport of fuel hydrocarbons (FHCs) released into California's diverse hydrogeologic settings and the impacts these releases may have on groundwater resources. This historical LUFT case analysis data set is perhaps the largest ever compiled that deals with impacts of FHC releases over an extended geographic area.

The initial objectives of the analysis of this best-available data are to answer several key questions:

- Do FHC plumes behave in predictable ways?
- What factors influence the length and mass of FHC plumes?
- To what extent are FHC plumes impacting California's groundwater resources?

The answers to these questions will aid in the identification of risk- and resource-management approaches that balance the cost of performing remediation against the anticipated benefits. Because there must be a pathway to a receptor to result in an impact to human health, one of the primary historical LUFT case analysis indices of potential risk impact is an estimation of benzene plume concentration and length. A further objective of the data analysis is to provide information about additional data that may be required to support improved risk- and resource-management decisions.

The historical LUFT case analysis data collection effort involved transcribing data, copying written documentation from LUFT case files, and entering data into an established electronic database. The variations of FHC fate and transport parameter between sites were summarized using simple, nonparametric graphical and numerical techniques.

Well locations were used in conjunction with groundwater time-series sampling of FHC and water level measurement to calculate benzene plume average concentrations and lengths, as well as groundwater gradients. This data has resulted in a series of plume average concentrations and lengths for each site, which allowed the analysis of changes in plume length, as well as groundwater gradient, with time.

Average LUFT site water chemistry and hydrogeologic characteristics results are summarized in this document. One of the most striking geologic characteristics of the LUFT cases analyzed in this study is the tendency for the sites to have shallow groundwater. Nearly half of the sites have mean groundwater depths of less than 15 ft. Most sites have multiple soil layers, and clay is fairly widespread.

The analyses of temporal changes in plume length and mass at each site are summarized. In general, plume lengths change slowly and tend to stabilize at relatively short distances from the FHC release site. Plume length estimations showed that averaged site plume lengths rarely

exceed about 250 ft. Benzene plume length tends to change slowly with time. Benzene plume average concentrations tend to decrease much more rapidly than plume lengths. While active remediation may help reduce plume benzene concentrations, significant reduction in benzene concentrations can occur with time, even without active remediation.

Individual or combinations of other hydrogeologic variables, such as groundwater depth or range, have little relationship to benzene plume lengths. This indicates that the plume length may not be predicted by consideration of hydrogeologic settings alone, and that there may be strong controlling variables that are not measured. These hypothetical plume-length controlling variables may be source mass and passive bioremediation rate. The data indicated that if FHC sources are significantly reduced or removed, plumes will likely heal themselves through passive remediation even if no active remediation is being performed.

The resulting estimated total volume of groundwater that may be impacted above a concentration of 1 ppb benzene is about 7,000 acre-feet. This volume of groundwater affected by LUFT benzene plumes is a very small proportion of California's total groundwater resource (0.0005%).

1. Introduction

1.1. Historical LUFT Case Analysis Goals

The primary goal of this study is to support revision of the leaking underground fuel tank (LUFT) corrective action process. California LUFT case historical data have been collected by state regulatory agencies for about ten years. Analysis of these data can provide information about the fate and transport of fuel hydrocarbons (FHCs) released into California's diverse hydrogeologic settings. The LUFT case data can also provide a basis for continuous evaluation of both the past and future impact LUFT releases may have on human health, the environment, and groundwater resources.

Several key questions that can be addressed by an analysis of the California LUFT case historical data are:

- Do FHC plumes behave in predictable ways?
- What factors influence the length and mass of FHC plumes?
- To what extent are FHC plumes impacting California's groundwater resources?

The answers to these questions will help identify risk- and resource-management approaches that balance the cost of performing remediation against the anticipated benefits.

The LUFT historical data set provides an unparalleled opportunity to evaluate the behavior of FHC plumes on a wide geographic scale. Many detailed studies are available that examine individual sites and the effects local hydrogeologic conditions have on FHC contamination fate and transport. The LUFT case historical data set provides a unique opportunity to draw broad regional conclusions about FHC fate and transport in California. A brief summary of the current understanding FHC fate and transport in the subsurface is available in **Appendix A**.

The historical LUFT case data can also be used as a basis to support implementation of a risk-based corrective action decision-making process. Analyses of past and current LUFT cases can be used to develop criteria to identify groups of sites in California where FHC releases behave differently and, thus, different risk management strategies may be employed. The LUFT historical data set can be used to generate probability frequency distributions of critical LUFT decision-making parameters such as groundwater depth or velocity. These probability frequency distributions can be used as a basis for the development of look-up tables that provide guidance to identify LUFT sites that pose a potential risk to human health or the environment (**Fig. 1**).

Continued LUFT case data analysis is key to implementing a risk-based corrective action approach. The historical LUFT data analysis can also provide information about additional data required to support improved risk and resource management. Information gaps and methods to fill these gaps need to be identified.

The historical LUFT case analysis was divided into three phases, i.e., exploratory, primary, and secondary analysis phases. This document reports the results of the exploratory and primary analysis phases.

2. Methods

2.1. Historical LUFT Case Data Collection

The historical LUFT cases used in this study were limited to leaking petroleum underground storage tank (UST) cases that meet the following criteria:

- The case must be an FHC leak site.
- The case must have been reported as affecting groundwater and have at least one monitoring well installed to collect groundwater data. Soil-only cases are not included in the sample.
- The case must at least be in the soil and water investigation phase. Eligible cases that reportedly impacted fractured rock hydrogeologic settings were excluded. These cases were excluded because FHC transport at fractured rock sites is complex, not well understood, and often poorly characterized.
- The case must be drawn from a master list of 5,700 eligible cases located within target counties in California (**Fig. 2**). The target counties were selected to represent a geographic cross section with large urban populations and a high proportion of the state's USTs. No more than 200 cases were selected within any one county. In some counties with less than 200 cases, all available cases were evaluated. Counties with a predominantly bedrock geology were excluded.

The historical LUFT case analysis data collection effort involved transcribing data, copying written documentation from LUFT case files, and entering the data into an established electronic database. A State Water Resources Control Board (SWRCB) team was assembled to travel to the appropriate oversight agency for each case identified. The original case file was evaluated, and case data transcribed and copied according to a standard checklist. This checklist was used as a basis for identifying the types of remediation applied at each site, e.g., over-excavation, or pump and treat.

A relational database structure was prepared to receive the case data. The historical LUFT case database structure is summarized in **Figure 3**. Well locations (x,y) were digitized based on site maps, while lithologic data based on well logs and FHC analytic results were entered directly into the database. As data input progressed, a series of quality assurance/quality control procedures were applied to provide data of known quality. Using relational database tools and documented procedures, entered data was further screened by a variety of checks, e.g., duplicate observations for the same well on the same date.

From the onset, it was recognized that there would be time and manpower limitations to this project; so, in addition to the SWRCB data entry team, the San Francisco Bay Regional Water Quality Control Board (SF RWQCB), and University of California (UC) LUFT team personnel, the Western States Petroleum Association provided funding to hire additional personnel to assist in the data entry under the supervision of SWRCB and SF RWQCB representatives.

2.2. Data Analysis Procedures

This study deals only with the impacts of FHCs and focuses on benzene as a conservative indicator of FHC fate and transport. Benzene is used because it is relatively more toxic and mobile than many of the other FHC constituents. Further, it is recognized that there are other compounds found in fuels that contribute to the overall risk to human health and the environment, but benzene, toluene, ethylbenzene, and xylenes (BTEX) are those that historically have the greatest amount of data available. Total petroleum hydrocarbon as gasoline (TPHg) measurements are also collected, but provide little information concerning risk, due to the non-specific nature of the measurement technique.

The principal statistical packages used to format and evaluate the data were SAS and S-Plus. S-Plus is a descendant of S, which was developed at AT&T's Bell Labs (Becker and Chambers, 1984; Becker *et al.*, 1988). Both packages provide a wide range of computational and graphical tools in an interactive environment.

The exploratory data analysis phase involved the iterative examination of data relationships using scatter diagrams and frequency distributions. Apparent outliers were reported to the data entry team, who checked the original data and made appropriate corrections as needed. The primary data set is maintained by the SWRCB UST Program staff.

Also during the exploratory data analysis phase, summary statistics for principal variables were developed, and data subsets were prepared to perform the primary and secondary analyses. These data subsets were used to calculate site spatial and temporal average benzene groundwater concentrations and estimates of plume length. Because there must be a pathway from LUFT FHCs to a receptor to result in an impact to human health or the environment, the primary historical LUFT case analysis indices of potential risk were average site groundwater benzene concentration and estimated plume length.

Monitoring-well spatial coordinates were used in conjunction with groundwater time-series sampling of FHC and water level measurements to calculate plume average benzene concentrations and lengths, as well as groundwater gradients. During the preliminary evaluation of plume lengths, it was found that many sites in the data set had a small number of installed monitoring wells and would, therefore, provide inadequate spatial resolution to model benzene plume lengths. Further, the spatial resolution was not constant because site characterization progressed in stages and the number of monitoring wells typically increased with time.

To calculate the best plume-length estimates possible and allow the analysis of changes in plume average benzene concentration and length with time, a site selection protocol was used to provide a data subset of well characterized sites used for modeling. To be regarded as well characterized for modeling and included in the plume trend analysis data subset, sites were required to have at least six monitoring wells installed. Each monitoring well was required to have groundwater depth sampling and benzene concentration data over at least eight observation periods.

The data from the plume trend analysis data subset sites provided the best possible estimations of spatially and temporally averaged plume benzene concentrations and plume lengths. For each site, a seven-day period was used to compute gradients and fit benzene plume length models for as many sets of observations as possible. This resulted in a time series of estimated plume lengths, average benzene concentrations, and groundwater gradients for each site.

Using this time series of plume data, changes in average plume benzene concentrations and estimated plume lengths were statistically evaluated during the plume observation period. The effects of remediation on changes in plume benzene concentration and length were statistically evaluated as well as the relationship between plume length and other measured hydrogeologic parameters. An estimate of the volume of groundwater affected by LUFT benzene plumes was used to evaluate the potential magnitude of the impact of LUFT FHCs on California's groundwater resources.

The variation of FHC fate and transport parameter among all the sites in the LUFT Historical Case Analysis data set were summarized using simple, nonparametric graphical and numerical techniques. Histograms and scatter diagrams form the predominant means of graphical presentation, whereas quantiles were used for numerical summaries. Quantiles are essentially the same as percentiles in that they give the value in a distribution below which a stated percentage of the data fall (Chambers *et al.*, 1983), e.g., the median is the 50% quantile. Quantiles were used rather than other typical numerical summaries, such as means and standard deviations, because their interpretation is not tied to any specific underlying distribution. The distributions of virtually all of the site-averaged quantities were decidedly non-Gaussian (not normally distributed), so it was desirable to employ distribution-free summaries.

2.3. Estimated Hydrogeologic Parameters

During the data analysis, it was often necessary to estimate LUFT site hydrogeologic parameters, such as hydraulic conductivity, because these data were either not available or not entered into the historical LUFT case data set. For example, for analyses that required a hydraulic conductivity determination, such as calculating a groundwater flow velocity at a site, borehole logs were used to identify soil lithologic types present at the site. An estimated hydraulic conductivity, derived from the literature (Freeze and Cherry, 1979) or from available local historical information (Bishop *et al.*, 1987), was assigned to each lithotype, and the average hydraulic conductivity for a depth interval was estimated. This type of approach was used where estimates of missing parameters were needed to complete an analysis. A variety of other derived estimates of hydrogeologic variables needed to evaluate FHC transport were also prepared. These are summarized in Table 1 and Appendix B.

2.4. Groundwater Gradient Calculations

Site groundwater gradients were estimated using multiple regression techniques to fit the observed groundwater surface elevations to a plane in three-dimensional (3-D) space. This simple linear gradient model predicts the direction and magnitude of the gradient relative to the coordinate system of the monitoring well locations. The lateral dimensions of most LUFT sites do not exceed more than a few hundred feet. In the absence of faults, groundwater sources, or sinks, local deviations in groundwater elevations are typically small, and a plane should represent a simple first-order approximation to the local water table surface. It should be understood that this simple approximation cannot be expected to accurately describe the shape of the water table if pump-and-treat type remedial activities or local infiltration is occurring at a particular site. Instead, these processes are likely to result in substantially more complex water-table surfaces, such as cones of depression or recharge mounds.

Table 1. Derived hydrogeologic parameters used during the analysis of historical LUFT case analysis data.

Average hydraulic conductivity = hydraulic conductivity (cm/s) was assigned for the following types of lithology:	
Asphalt	1×10^{-10}
Clay	1×10^{-7}
Fill	1×10^{-3}
Gravel	1×10^{-1}
Rock	1×10^{-10}
Sand	1×10^{-3}
Silt	1×10^{-5}
The average hydraulic conductivity is the depth-weighted average across a borehole's saturated zone screened interval.	
Groundwater flow velocity = effective groundwater flow velocity during a given date (ft/yr) = hydraulic conductivity $\times 1,034.6$ ft/yr. Note: groundwater is assumed to flow preferentially through higher zones of hydraulic conductivity (1×10^{-3} cm/s = $1,034.6$ ft/yr).	
Groundwater range = maximum groundwater depth minus minimum groundwater depth (ft).	
Number of layers = number of different lithology layers within a given borehole.	
Plume aspect ratio = plume length / plume width.	
Plume length, erf = estimated groundwater plume length for 10 part per billion (ppb) benzene, using error function (erf) model (ft).	
Plume length, exp = estimated groundwater plume length for 10 ppb benzene, using exponential (exp) model (ft).	
Plume volume = plume length \times plume width \times plume depth.	
Plume depth = groundwater depth range + (plume length \times estimated dispersion coefficient). Estimated dispersion coefficient = 0.1 (Anderson, 1984).	
Sand and gravel thickness = total thickness of sand and gravel layers within a given borehole (ft).	
Site observation period = maximum sample date minus minimum sample date (yr).	
Site gradient = slope of a plane fit through a series of groundwater surface elevation measurements on a given observation date (ft/ft).	
Site size = longest diagonal distance of a rectangle formed by the minimum and maximum (x,y) borehole coordinates (ft).	
Standard deviation of gradient orientation = standard deviation of groundwater direction averaged across observation dates at a given site (deg).	

2.5. Evaluation of Spatial Distribution of Hydrogeologic Parameters Affecting FHC Fate and Transport

During the primary data analysis phase, the lithologic profiles and hydrogeology at the LUFT sites were evaluated. In a number of instances, this involved calculating site-averaged quantities, e.g., depth to groundwater and thickness of clay layers, from observations and point measurements taken from within boreholes. Site averages were calculated using a simple spatial interpolation method based on Delaunay triangulation (Isaaks and Srivastava, 1989). The region bounded by the boreholes (or convex hull) is divided into triangles, with a borehole at each

vertex. The spatial variations within each triangle are assumed to be planar, making the area average of the quantity of interest within each triangle simply the average of the values at the vertices. An overall site average is then calculated by using a weighted sum of the values for each triangle, weighting by the relative areas of the triangles.

This interpolation technique produces a surface that is continuous, but not differentiable at the edges of the triangles. Other more complex interpolation techniques could remove this problem, but the LUFT Team felt that the additional complexity was not warranted. The number of borehole points per site was usually small (ten or less), and the desired quantity was a site average rather than values at any specific points. Note that the "site average" is really calculated for the portion of the site bounded by the boreholes. This was done because extrapolating beyond the convex hull of the data points can produce misleading results, even with a linear interpolator, and because it was not clear how to define site boundaries in any other reasonable fashion with the available information.

Initially, a series of geologic site characteristics were selected as potential vadose FHC fate and transport predictors. These site characteristics were spatially and time-averaged depth to groundwater, average clay thickness, number of soil layers, number of clay layers, percentage of site area with clay, and proportion of site area covered by asphalt. The key variable that was expected to be differentiated was estimated FHC.

Two different two-dimensional (2-D) groundwater contamination models were used to fit observed groundwater contamination data and thereby estimate plume length. A pilot study was performed by the UC LUFT Team to demonstrate a microcomputer methodology to estimate plume length. The pilot study used a rudimentary exponential decay model to describe the spatial distribution of FHCs.

The pilot study plume lengths compared well with plume lengths generated by best professional judgment, as well as with those produced by a commercial isocontouring package. Based on the pilot study results, plume dimensions were estimated using both a linearized form of the pilot study exponential model and a nonlinear error function model. An overview of the implementation of the plume models and details on their form is provided in **Appendices B, C, and D**. The estimations of plume length are intended to be used during analysis of available data and not intended as a widely applied methodology for characterizing plumes at individual sites.

Using the plume trend analysis data subset, estimated plume lengths were calculated using both a plume length detection limit of 1 ppb benzene and a plume length practical limit estimation of 10 ppb benzene. A robust estimate of plume length is needed when evaluating plume spatial changes with time. The FHC analytic data can be quite variable, and benzene plume boundary estimations at concentrations less than 10 ppb can be strongly influenced by this variability. Estimated plume lengths using 1 ppb benzene were used only during the conservative estimation of plume volume. During the evaluation of other relationships involving the use of plume length, the practical limit of plume length estimation was used.

2.7. Temporal Analysis of Benzene Plume Average Concentration and Length

Average benzene concentrations were calculated for each site. Spatial averages were estimated using the planar triangular interpolation technique (described above) for log10 of benzene concentrations. Both the time averages and trends in spatial averages were calculated using robust M-estimates. This technique uses weighted least squares with weights iteratively calculated, with the objective of limiting the influence of outliers. In looking through the plume data, it became clear that outliers were common and could result from a number of different sources, e.g., the variable nature of the concentration measurements, even on a log scale, or variations in sampling, such as sampling nondetect wells more frequently than those showing high concentrations. Confidence intervals and significance tests for the robust estimates were carried out using a Monte-Carlo resampling method, which involves repeatedly drawing samples from the data and recalculating the statistics of interest to build up a distribution for the test statistics. This process minimizes the influence of outliers during the analysis.

Using the plume trend analysis data subset, sites with significant log-linear trends in plume average benzene concentration or linear trends in length were identified, and the significance or lack of significance was treated as a categorical variable for further comparison with other site variables. Logistic regression (McCullagh and Nelder, 1989; Chambers and Hastie, 1992) was used to estimate the effects of potential FHC fate and transport predictors on the probabilities of getting a significant trend. This technique models the logarithm of the odds ratio ($p/[1-p]$) as a linear function of the predictors, which can either be continuous, e.g., mean depth to groundwater, or categorical, e.g., whether pump and treat was employed. One advantage of predicting the logarithm of the odds ratio is that the resulting probability estimates will always be between zero and one. This type of model shares many attributes of ordinary linear models, and the overall significance, as well as the importance of the contributions of each predictor, can be determined, at least approximately.

3. Results

3.1. Groundwater Chemistry

Temporally and spatially averaged site groundwater chemistry results for all cases in this study are summarized in Table 2. Scatter plots of benzene versus toluene, ethylbenzene, total xylenes (BTEX); and total petroleum hydrocarbons as gasoline (TPHg) are shown in Figure 4. Table 3 summarizes the results of a correlation analysis of benzene versus BTEX and TPHg.

Within the historical LUFT case analysis data set, few measurements of inorganic ions which may be indicative of biodegradation were found. A total of 637 O_2 observations representing 41 sites were found in the data set. No measurements of pH, redox potential, NO_3^{-1} , Mn^{+2} , SO_4^{-2} , or methane were available. The correlation between measured O_2 and TPHg was evaluated for each of the 41 sites with available data. Sixty-three percent of the sites showed an relationship between increasing TPHg and decreasing O_2 groundwater concentrations. The significance of these relationships was not assessed due to the high variability observed in the O_2 measurements in monitoring wells in which FHCs were not detected. The 50% quantile of these observations was unusually low—3.8 mg/l dissolved O_2 .

3.2. Hydrogeologic Characteristics

Average site hydrogeologic characteristics are summarized in Table 4.

One of the primary characteristics of the LUFT cases analyzed in this study is the tendency for the sites to have shallow groundwater (Figs. 5–7). Mean depth to groundwater is averaged over time and space, whereas maxima and minima reflect range-over-time averages spatially. Nearly half of the sites have mean groundwater depths of less than 15 ft. Considering that about one-quarter of the sites have a groundwater minima of 7.5 ft or less, it is clear that in a large fraction of cases the underground tanks were in direct contact with the groundwater at least part of the time.

Table 2. Summary of site-, time-, and spatially averaged groundwater concentration data. Water chemistry data was temporally averaged over each site's history.

	Number of sites	50% quantile	90% quantile	99% quantile
Benzene, ppb	1,094	22.7	362	3,000
Toluene, ppb	275	10.4	175	1,213
Ethylbenzene, ppb	275	17.7	227	1,214
Xylene, total, ppb	276	24	311	2,088
Total petroleum hydrocarbon, gasoline, ppb	1,042	871	7,343	36,000
Free product thickness, ft	450	0.099	0.76	2.18

Table 3. Correlation of benzene groundwater concentration analytical results to toluene, ethylbenzene, total xylenes, and total petroleum hydrocarbon–gasoline (TPHg) groundwater concentration analytic results.

	R ² for Y = benzene ^a
Toluene	0.790
Ethylbenzene	0.720
Xylene, total	0.748
TPHg	0.578

^a R² is proportion of the variability in the benzene groundwater concentrations that is predicted by measuring toluene, ethylbenzene, xylene, or TPHg.

The geologic structure of the LUFT sites was characterized by the total number of layers (Fig. 8), number of layers above the mean groundwater table (Fig. 9), total thickness of clay layers (Fig. 10), and thickness of clay layers above the mean groundwater table (Fig. 11). Most

Table 4. Summary of site average hydrogeologic characteristics.

	Number of sites	50% quantile	90% quantile	99% quantile
Hydraulic conductivity ^a , cm/s	855	0.00082	0.023	0.080
Total number of layers ^a	993	6	11	19
Sand and gravel thickness ^a , ft	992	7.9	19.4	48.4
Groundwater depth ^b , ft	1,134	15.2	52.3	97.3
Groundwater depth range ^b , ft	1,134	3.5	9.7	22.7
Maximum depth to groundwater, ft	1,134	17.6	56.0	101
Minimum depth to groundwater, ft	1,134	13.0	50.0	88.6
Groundwater gradient ^b , ft/ft	686	0.0076	0.042	0.30
Standard deviation of groundwater ^b gradient orientation, deg	601	35	138	187
Groundwater flow velocity ^c , ft/yr	686	7.8	73.6	310
Site observation period, yr	1,184	2.9	5.2	7.2

^aSpatially averaged across site.^bSpatially and temporally averaged across site.^cPrimary plume pathway assumed to be sand and gravel, and hydraulic conductivity assumed to be 0.001 cm/s.

sites have multiple soil layers, and clay is fairly widespread. Shallow groundwater limits the number of layers between the ground surface and groundwater, but nevertheless, 75% of the sites have at least two layers. Of all layers at all sites, 29% are sand, 26% clay, 17% silt, and 6% gravel, while 13% are asphalt and 7% fill. Rock lithotypes were intentionally excluded.

3.3. LUFT Plume Characteristics

Estimated plume lengths were calculated using the error-function model. This model was used as the primary estimator of plume spatial distribution because it was found to be less sensitive to outlier data and typically produced better fits to the data than the exponential model (see **Appendix B**). Plots of error-function-model estimated plume lengths and hydrogeologic characteristics are shown in **Figure 12**. Average site-modeled benzene plume lengths are summarized in **Table 5**. The estimated volume of water that may be affected by benzene was derived from the 95% quantile result for all site average plumes with concentrations greater than 1 ppb. This 95%-quantile plume volume was found to be 2.3×10^5 gal (0.70 acre-feet).

3.4. Temporal Changes in Average Benzene Concentration and Plume Length

Table 6 summarizes the results of the trend analysis of changes in the log of average site benzene concentrations with time. This analysis was performed on the 271 sites identified as meeting the trend analysis data quality criteria. The table shows the results of testing for the

Table 5. Summary of modeled benzene groundwater plume site average characteristics.

	Number of sites	50% quantile	90% quantile	99% quantile
Average site 10 ppb benzene plume length, ^a exponential model, ft	271	130	306	915
Average site 10 ppb benzene plume length, ^a error function model, ft	271	101	261	550

^aPlumes lengths calculated using sites with at least six monitor wells and eight observations per monitor well.

significance of observed trends in the log of average site concentrations. A majority of these sites show significant decreasing trends in average plume benzene concentration.

Actual values of the significant negative concentration trends vary widely, with 10% and 90% quantiles -0.0020/day to -0.0004/day, and a median of -0.0008/day. Since concentration trends are log-linear, the inverse of these numbers can be interpreted as the amount of time required for average concentrations to decrease tenfold (characteristic time scales). The range is from about 500 to 2500 days (1.5 to 7 yr) with a median of 1175 days (3.2 yr). The significant positive concentration trends are generally smaller in absolute magnitude, resulting in longer characteristic time scales. The 10% and 90% quantiles are 0.0003/day and 0.0016/day, with a median of 0.0004/day. These numbers translate into characteristic time scales for tenfold increases in average plume benzene concentration of 600 to 3800 days (1.7 to 10.5 yr) and a median of 1725 days (4.7 yr).

Changes in benzene plume length appeared to be mainly linear, in contrast to the logarithmic behavior of plume concentrations, so linear trend models were fit to the length data. Results of the trend analysis of benzene plume lengths are summarized in Table 7.

Table 6. Results of the test for significant trends in the change in average site concentrations with time.

	Number of sites	Percent
Decreasing benzene concentration	161	59.4
Increasing benzene concentration	21	7.7
No significant trends	89	32.8

Table 7. Results of the test for significant trends in the change in site plume lengths with time. Plume lengths were defined using a benzene concentration of 10 ppb.

	Number of sites	Percent
Decreasing plume length	89	32.8
Increasing plume length	22	8.1
No significant trends	160	59.0

An important result is that substantially fewer sites show negative length trends than negative concentration trends. The number of sites showing positive trends are about the same for concentrations and lengths, and many more sites have no length trends rather than no concentration trends.

The 10% and 90% quantiles for the sites with significant negative length trends are -0.094 ft/day and -0.014 ft/day (10.5 days/ft and 73.5 days/ft), and the median is -0.037 ft/day (27 days/ft). Since the length trends are linear, it is not possible to compare them directly to the logarithmic concentration trends. A roughly comparable time scale can be determined by calculating the length of time required for plume lengths to decrease (linearly) to 10% of their initial values. These time scales range from about 4 yr to about 15 yr, with a median of about 9 yr, so decreases in plume length are generally slower than changes in concentration. The magnitude of significant positive length trends was roughly comparable to that of significant negative trends, although a small number of sites (five) had rapidly increasing lengths, greater than 0.1 ft/day.

The 89 sites with no significant concentration trends were further subdivided into two groups based on average benzene concentrations. The first group consisted of the 47 sites that have average concentrations less than 10 ppb, and most of these (42) have averages less than 5 ppb. The median concentration for this group is about 1.6 ppb. Furthermore, average benzene plume lengths for these sites are generally low, with a median of 35 ft and a 90% quantile of 70 ft. Only three of these sites show increasing trends in benzene plume length, and 15 show decreasing length trends. It seems reasonable, therefore, to characterize this group of sites as having essentially "exhausted" or inactive benzene plumes.

The remaining group of 42 sites without significant trends all have average concentrations greater than 10 ppb. Almost two-thirds (27 of 42) have benzene concentration averages greater than 50 ppb, while 18 have average benzene concentrations greater than 100 ppb. Plume lengths are generally longer, as well, with 75% greater than 60 ft and 25% greater than 135 ft. Not many sites have increasing plume lengths (four of 42), but not many have decreasing length trends either (also four of 42). Most of these sites appear to have plume lengths that have stabilized at relatively large values and concentrations that indicate that the plumes still contain substantial amounts of benzene.

Table 8 shows the site frequencies for the different average benzene concentration and plume length trend categories.

Note that a large proportion (83/89) of the sites with negative length trends have either negative concentration trends or low concentrations. Conversely, just over half (84/161) of the sites with negative concentration trends have no length trends.

3.5. Impacts of Remediation on Plume Length and Average Benzene Concentration

A set of analyses was performed to examine the factors distinguishing sites with benzene plume concentrations that showed no trends and low average concentrations (the "exhausted plume" concentration class) from the remaining sites. Only one variable, depth to groundwater, had a significant impact on the probabilities of a site being in this class. Sites with deeper groundwater generally have smaller probabilities of low benzene concentrations. For example,

12.0% of the 142 sites with groundwater deeper than 12 ft fall into this class, compared to 23.3% of the 129 sites with groundwater shallower than 12 ft.

An alternative way to define "exhausted plume" sites may be based solely on time-averaged plume concentrations. Using this criterion, 63 of the 271 sites (23.2%) having time-averaged benzene concentrations not significantly greater than 1 ppb were selected, regardless of whether or not they showed a trend. The variables, over-excavation and depth to groundwater, play important roles in distinguishing sites with "exhausted plumes" from the rest. **Table 9** summarizes the impact of different combinations of these two variables on the probabilities of a site having an average benzene concentration less than 1 ppb. Note that for shallow sites that are over-excavated, the chances of having average benzene concentrations not significantly greater than 1 ppb are more than twice as great as in any of the other situations.

A second set of analyses focused on the 224 sites that had either significant increasing or decreasing trends or high benzene concentrations that were stable with time (no significant trends). Tests were carried out to determine if each of the remediation treatment variables or minimum depth to groundwater had an impact on the relative frequencies of the three remaining categories (positive trends, no trends but high concentrations, negative trends). Either pump and treat or over-excavation increased the probability of having a negative trend, from 0.72 to around 0.77, and the combination of both increased the probability to 0.83. None of these differences are statistically significant, however. Minimum depth to groundwater also has a modest insignificant impact, with shallower sites showing greater probabilities of decreasing trends.

Table 8. Frequency of LUFT study sites that fall into average plume benzene concentration and length trend analysis categories.

	Plume length trends			Total
	Positive	None	Negative	
Significant positive plume concentration trend	6	13	2	21
Insignificant trend, average plume concentration > 10 ppb	4	34	4	42
Significant negative plume concentration trend	9	84	68	161
Insignificant trend, low average plume concentration < 10 ppb	3	29	15	47
Total	22	160	89	271

Table 9. Effect of groundwater depth and over-excavation on the probability of observing a site average plume benzene concentration of less than 1 ppb.

	No over-excavation	Over-excavation
Groundwater depth < 12 ft	0.185	0.432
Groundwater depth > 12 ft	0.209	0.214

Turning to the 208 sites that show time-averaged benzene concentrations significantly greater than 1 ppb, remediation treatment technique and groundwater depth were found to have significant impacts on the probability for significantly negative log-linear trends in concentration. Pump and treat had the greatest impact, with 39 of 53 (73.6%) of the pump-and-treat sites showing significant negative trends, whereas there were 87 of 155 (56.1%) of those sites without pump and treat still showing significant negative trends. Soil vapor extraction also had an impact, increasing the probability of a negative trend in concentration from 0.58 to 0.66, but there is no evidence of an additional benefit from soil vapor extraction in sites where pump and treat was also carried out. Site over-excavation, on the other hand, does show a significant benefit in combination with pump and treat. **Table 10** shows the probabilities of a significant negative trend when the different combinations of the two treatments are applied.

There is also an indication that depth to groundwater plays a role when neither over-excavation nor pump and treat are employed, with increasing chances of significant negative trends in average site benzene concentrations at sites with deeper groundwater. For example, 65% of the sites with neither treatment reported and with groundwater deeper than 25 ft show decreasing trends, while only 49% of the shallower untreated sites show decreasing trends. This appears to be a second-order effect when compared to the treatment variables.

Another rather subtle result is that the benefit of the remediation treatment option appears to vary depending on initial benzene concentrations. In general, the probability of finding a negative trend in average site benzene concentration increases with increasing initial benzene concentrations. In 46 of 106 sites (43.4%) where the initial area-averaged benzene concentrations were less than 100 ppb, significant decreasing trends were found, whereas 80 of 102 sites (78.4%) with initial concentrations greater than 100 ppb showed decreasing trends. However, the impact of pump and treat on the probability of a decreasing trend is greater for the sites with lower initial concentrations. At low concentration sites, pump and treat increases the probability of having negative average benzene concentration trend by roughly a factor of two, while it has essentially no impact on probability at high concentration sites.

An analysis of plume length categories shows that none of the remediation treatment variables have a significant impact on the relative frequencies of the different categories. Depth to groundwater does have a significant relationship with the probability of observing increasing lengths, with deeper sites showing higher probability of increasing plume lengths. Estimated probability ranges from less than 0.05 for very shallow sites (minimum depth < 7 ft) to more than 0.20 for deep sites (depth > 60 ft).

Table 10. Effect of two site remediation techniques on the probability of observing a decrease in average plume benzene concentration with time.

	No over-excavation	Over-excavation
No pump and treat	0.524	0.640
Pump and treat	0.711	0.800

4. Discussion

4.1. Do FHC Plumes Behave in Predictable Ways?

Based on the preceding LUFT case analyses, a plume's geometry tends to change slowly with time. In general, plume lengths change slowly and tend to stabilize at relatively short distances from the FHC release site. Error-function-model estimations indicate that average site plume lengths rarely extend beyond about 250 ft. Plume masses tend to decrease more rapidly than plume lengths change. Active remediation helps reduce plume mass, but even without pump and treat or other active remediation, there is a high probability of significant mass reduction with time.

As a result of the analysis of temporal changes in plume average concentration and length, a hypothetical model of a plume life cycle can be proposed (Fig. 13). This model assumes that there are four phases in a plume's life history. Phase I is a plume's growth phase. An active source is present in which FHC free product is in contact with the groundwater, FHCs dissolve into the groundwater, and the dissolved FHCs are transported downgradient. As the dissolved FHC plume moves with the groundwater, it spreads, and part of the FHC mass sorbs onto (attaches to) soil particulates and part is lost through volatilization into the air. The sorption retards the movement of the plume relative to the groundwater flow. As long as there is continuing mass input from the active source, the plume length and mass, as indicated by average plume concentration, will continue to grow.

During our trend analyses, sites with phase I plumes can be identified by a significant increase in both plume length and mass with time. Tables 6 and 7 indicate that about 8% of the well characterized LUFT sites in this study appeared to be in this plume life history phase.

At a short distance from the source, a growing plume may stabilize and enter phase II in its life history (Buscheck *et al.*, 1993; McAllister and Chiang, 1994). Sites with phase II plumes can be identified by insignificant temporal changes in length and mass along with relatively high average plume concentrations. Results of this study indicated that 16% of the well characterized sites were found to have stable average benzene concentrations greater than 10 ppb, while 42% of the sites had stable plume lengths. This finding may be expected because plume concentrations tend to decrease more rapidly and frequently than plume lengths, and there is a greater probability of finding a stable plume length than a stable plume concentration.

During phase II, a zone of FHC passive bioremediation is established in which mass is removed from the plume and the plume stops growing. The FHC mass contributed to the plume from the active source is removed in the passive bioremediation zone. This removal is due to the digestion of FHC by subsurface microorganisms (Ghiorse and Wilson, 1988; Baedecker *et al.*, 1993; NRC, 1994; Borden *et al.*, 1995). Appendix A summarizes the passive bioremediation process.

Once an active source is depleted or removed, a plume enters phase III. During phase III, the plume's length decreases slowly while the mass decreases rapidly. Plume mass is reduced due to either active remediation, such as pump and treat, or passive bioremediation, or both. The FHCs sorbed onto the soil particulates tend to inhibit changes in plume length because even if the groundwater concentrations of FHC become low, the soils will desorb FHCs slowly back into

groundwater, and a measurable plume length will still be present (Bear *et al.*, 1994). The lingering plume length is defined by the soils with residual sorbed FHCs. During phase III, a plume's mass and average benzene concentration decrease exponentially. A majority (59%) of the well characterized sites used in this study were found to have decreasing average benzene concentrations, and 33% were found to have decreasing plume lengths.

As the plume mass reaches a relatively low residual mass, the plume reaches the end of its life cycle and enters phase IV. Sites with phase IV plumes can be identified by insignificant temporal changes in length and mass along with average plume concentrations not significantly greater than 1 ppb. Phase IV plumes may be considered to be "exhausted plumes." They may still have a measurable plume length, but the mass has been reduced to a low amount, and the rate of mass reduction has slowed. Passive bioremediation will continue to remove mass at a lower rate because the FHC food source has been diminished. Active remediation will typically not be cost effective at this point. About 17% of the well characterized sites in this study could be considered to have "exhausted plumes."

4.2. What Factors Influence the Length and Mass of FHC Plumes?

Although plume length does not correlate with groundwater depth, sites in this data set with shallow groundwater have a higher probability of groundwater impact. This may be a result of the hydrogeologic settings within the counties chosen for the historical LUFT case data set. Gas stations typically are clustered in urban areas, and most of the heavily populated counties selected for this study are located in the Coastal Range sedimentary or valley alluvium hydrogeochemical provinces (Thomas and Phoenix, 1976). These provinces typically have shallow groundwater, and the historical LUFT case analysis study may reflect this.

Individual or combinations of other hydrogeologic variables have little apparent relationship to plume characteristics. Correlations among a variety of hydrogeologic variables and plume length show no indications of interaction. Transport indices that in theory should effect plume length, such as groundwater flow velocity, show no correlation. There are four possibilities to explain the observed random scatter in plume lengths relative to a variety of hydrogeologic parameters.

1. There may be strongly controlling variables that are not measured. Two possible variables may be source mass and biodegradation rate. The possibility that one of the variables is source mass is supported by the finding that over-excavation can reduce the likelihood of benzene getting into the groundwater in high concentrations. Further, it was found during LUFT case data collection that information regarding the magnitude of FHC release sources are typically poor.

The possibility that biodegradation rate is a controlling variable is indicated by the finding that greater than 50% of the sites show decreasing plume concentration trends even if no treatment was reported. Information regarding the activity of bioremediation is also typically lacking.

2. The data on hydrogeologic variables may be poorly taken, and the scatter in the plume-length-correlation results may be due to random sampling noise. This possibility is unlikely. The historical LUFT case analysis data set represents a very large amount of

best available data, and the size of this data set would tend to minimize the influence of sampling noise.

3. A cyclic change in hydrogeologic variables may result in delayed effects in benzene plumes. For example, changes in groundwater surface elevation may result in changes in observed plume length, but only after some delay in time. Site-wide averages that integrate information across different observation times may mask effects that lag behind a causal event. Comparison within a short observation period may also miss effects out of phase or that lag.
4. Each site is unique and complex. The above three possibilities are not mutually exclusive. Conceivably all four possibilities are in effect to a differing degree at each site, e.g., the subsurface environment is very complex and each site has a unique controlling set of variables.

Scales of heterogeneity may be at issue in grouping sites into classes. For terrestrial soil samples, the composition of natural materials is typically heterogeneous on a small spatial scale, homogeneous on a larger spatial scale, and heterogeneous on an even larger spatial scale (Campbell, 1978). The LUFT historical case data may represent a regional spatial scale in which the hydrogeologic properties are in effect homogeneous, and thus there is little discrimination between sites. If there is a jump in scale from a regional perspective to a statewide perspective, there may be evidence of site-class distinctions. For example, if the spatial scale of the LUFT data evaluation is statewide and fractured rock settings were included, there may be distinctions between groups of sites, e.g., alluvial versus fractured rock.

Overall, an important observation to come out of these analyses is that the results are quite sensitive to moderate changes in the way plume characteristic categories are defined. As a result of this instability, any "statistically significant" findings that are observed during this primary analysis phase must be interpreted with caution. Neither depth to groundwater nor any of the remediation treatment variables have relationships with concentration or length trends that are strong enough to show up as consistent signals throughout all the analyses.

There are a few tentative conclusions that can be drawn from these analyses, however. First, it appears that over-excavation can reduce the likelihood of benzene getting into the groundwater in high concentrations, especially in sites with shallow groundwater. Second, once benzene does get into the groundwater in significant concentrations, there is a greater than 50-50 chance that it will show signs of diminishing without any treatment. Application of pump and treat may increase the chances of significantly decreasing trends in average plume concentration, and over-excavation may further increase the chances. Finally, plumes at sites with very shallow groundwater almost never show increasing lengths, while those at sites with relatively deep groundwater are more likely to grow.

Once groundwater contamination has occurred, the subsurface environment displays a plume length buffering capacity that may stabilize plume lengths, depending on the magnitude of the source mass. If sources are significantly reduced or removed, plume mass will likely be reduced through passive bioremediation, even if no active remediation is being performed.

4.3. To What Extent Are FHC Plumes Impacting California's Groundwater Resources?

To estimate the volume of water that may be affected by benzene plumes in California, the 95% quantile result (0.70 acre-feet) derived from the probability frequency distribution for site average 1 ppb plume volume was applied to the approximately 10,000 LUFT cases that have reportedly affected groundwater. The resulting estimated total volume of groundwater that may have been impacted above a concentration of 1 ppb benzene is approximately 7,060 acre-feet. The estimated total basin storage capacity in California is 1.3 billion acre-feet (CDWR, 1975). The proportion of the estimated total basin storage capacity that may be affected by LUFT benzene plumes can be calculated to be 0.0005%.

4.4. How Are Data Used in LUFT Decision-Making Approach?

The idea that complexity of site uniqueness may be high in the group of sites represented in the LUFT historical case data set is an important consideration. From one point of view, this could be seen as a regulatory difficulty because it requires very site-specific regulatory judgment and decision making.

On the other hand, the hydrogeologic setting in which a majority of LUFT cases typically have occurred, and will most likely occur in the future, can be used to advantage. If the hydrogeologic settings represented within the LUFT historical case data set are considered to represent a single class of sites, there may be predominant effects that can be used to guide a statewide or broad, regional decision-making framework to manage a group of unique sites. These dominant effects may include the findings that (1) average site benzene concentrations have a high probability of decreasing even if no treatment is attempted, (2) benzene plume lengths rarely extend beyond 250 ft, and (3) over-excavation at sites with shallow groundwater improves the probability of observing a decrease in plume average concentration.

The American Society for Testing and Materials/risk-based corrective action (ASTM/RBCA) bases its tiered approach for evaluating FHC effects on groundwater on U.S. Environmental Protection Agency guidance (U.S. EPA, 1990), as well as on models from other sources (Jury *et al.*, 1983; Johnson and Ettinger, 1991). **Table 11** shows the parameters used in the ASTM/RBCA tier-one and tier-two decision-making process, as well as sources for these data, including the historical LUFT case analysis database.

The current, risk-based target action screening levels (TASLs) found in ASTM/RBCA are based on a series of specific default values. These default values can be replaced by probability distribution functions (PDFs) prepared using the LUFT historical case data. PDFs of the specific RBCA decision-making parameters, propagated through either a Monte-Carlo method or through a convolution integral, will give realistic risks based on cumulative distributions and allow the decision maker to properly assess uncertainty associated with a site's risk. The PDFs developed can be used to set up California's Tier One TASL soil and groundwater concentrations, and the site's risk level can then be compared to the cumulative risk distributions to determine its action priority level, as well as determine the amount of site data that must be gathered to increase the confidence level of the overall risk estimate. Use of these PDFs will allow for various levels of risk to be incorporated into the decision-making approach. When specific site information is

available, the historical LUFT case analysis database can be used to supplement available site information during tier-two evaluations.

4.5. Other Needed Data

A summary of emerging technologies that are applicable to the LUFT cleanup process is provided in **Appendix E**.

Of particular interest to an RBCA approach is the lack of data regarding soil organic carbon content. Initial sensitivity studies indicate that soil organic carbon content is an important parameter. Along with the carbon-water sorption coefficient, which is chemical specific, these two parameters make up the soil-water distribution coefficient. This coefficient may have a strong effect on predicting the distributions of FHC plume lengths and mass.

As part of a revised LUFT cleanup process, routine measurement of inorganic ions are very important. These measurements are inexpensive and can often be performed in the field. These measurements in conjunction with a determination of plume stability can form an *a priori* argument that biotransformations are occurring and can be utilized as part of a remediation and risk-management strategy. A lot of variability was observed in the O₂ measurements in monitor wells in which FHCs were not detected, and the 50% quantile of these observations was unusually low, 3.8 mg/l dissolved O₂. This may indicate that the anaerobic zone of plume extends beyond the area within a plume where FHCs are present, and care must be taken when establishing background measurements used during an evaluation of passive bioremediation processes.

Table 11. Basic hydrogeochemical parameters necessary to create RBCA target action screen levels. Also shown are other possible data sources used to support the ASTM/RBCA decision-making process.

Parameter Description	Symbol	Units	PDF	Data source
Soil concentration	C _s	mg/kg		1, 2, 3
Groundwater concentration	C _L	mg/kg		2, 3
Diffusion coefficient, air	D _g	cm ² /s		4
Diffusion coefficient, water	D _l	cm ² /s		4
Henry's law constant	H	—		4
Solubility	S	mg/kg		4
Distribution coefficient	k _d	ml/g		4, 5
Decay rate constant	λ	1/day		2, 5, 6
Volumetric water content	θ _w	—	*	2, 6, 7, 8
Soil porosity	θ _s	—	*	2, 6, 7, 8
Dry soil bulk density	ρ _b	g/cm ³	*	2, 7, 8
Fractional organic carbon content	f _{oc}	—	*	2, 4, 5
Groundwater depth	d _{gw}	cm	*	2, 3
Groundwater fluctuation	σ _{gw}	cm	*	2, 3
Groundwater gradient	h	—	*	2, 3
Hydraulic conductivity	k	cm/s	*	2, 4, 5
Recharge rate	R	cm/s	*	5, 6
Averaging time for exposure	AT	yr		6
Body weight	BW	kg	*	9
Exposure duration	ED	yr	*	10
Exposure frequency	EF	days/yr	*	10
Soil ingestion rate	IR _{soil}	mg/day	*	9
Inhalation rate	IR _{air}	m ³ /day	*	11
Water ingestion rate	IR _w	l/day	*	9

* Probability distribution function (PDF) for use in California Tier-One analysis.

- | | |
|---|--|
| 1 Tier One site-specific investigation | 7 Future LUFT data requirement |
| 2 Tier Two site-specific investigation | 8 Schwalen <i>et al.</i> (1995) DTSC study |
| 3 California LUFT historical case analysis (1995) | 9 Finley <i>et al.</i> (1994) |
| 4 Chemical specific | 10 Layton <i>et al.</i> (1993) |
| 5 California LUFT demonstration site studies (proposed) | 11 Layton (1993) |
| 6 Various literature, including EPA sources | |

Figures

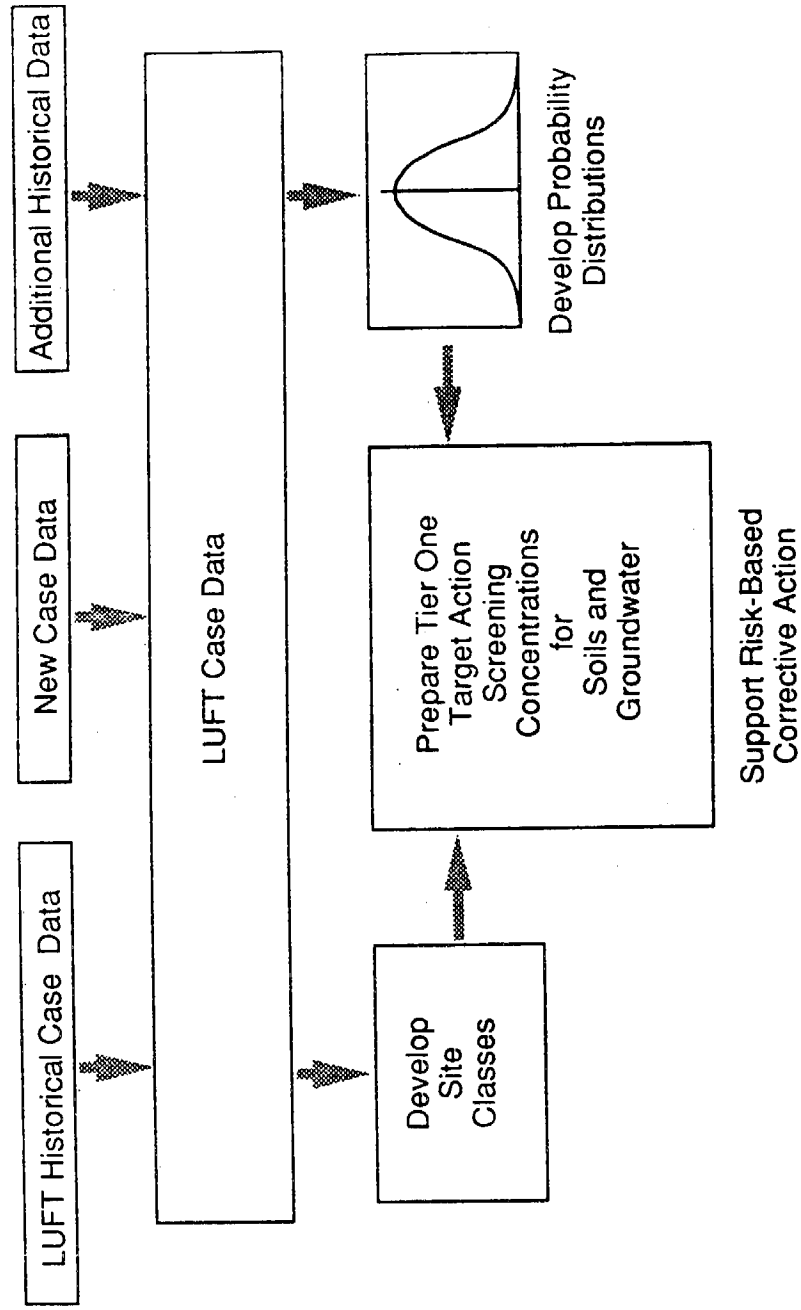
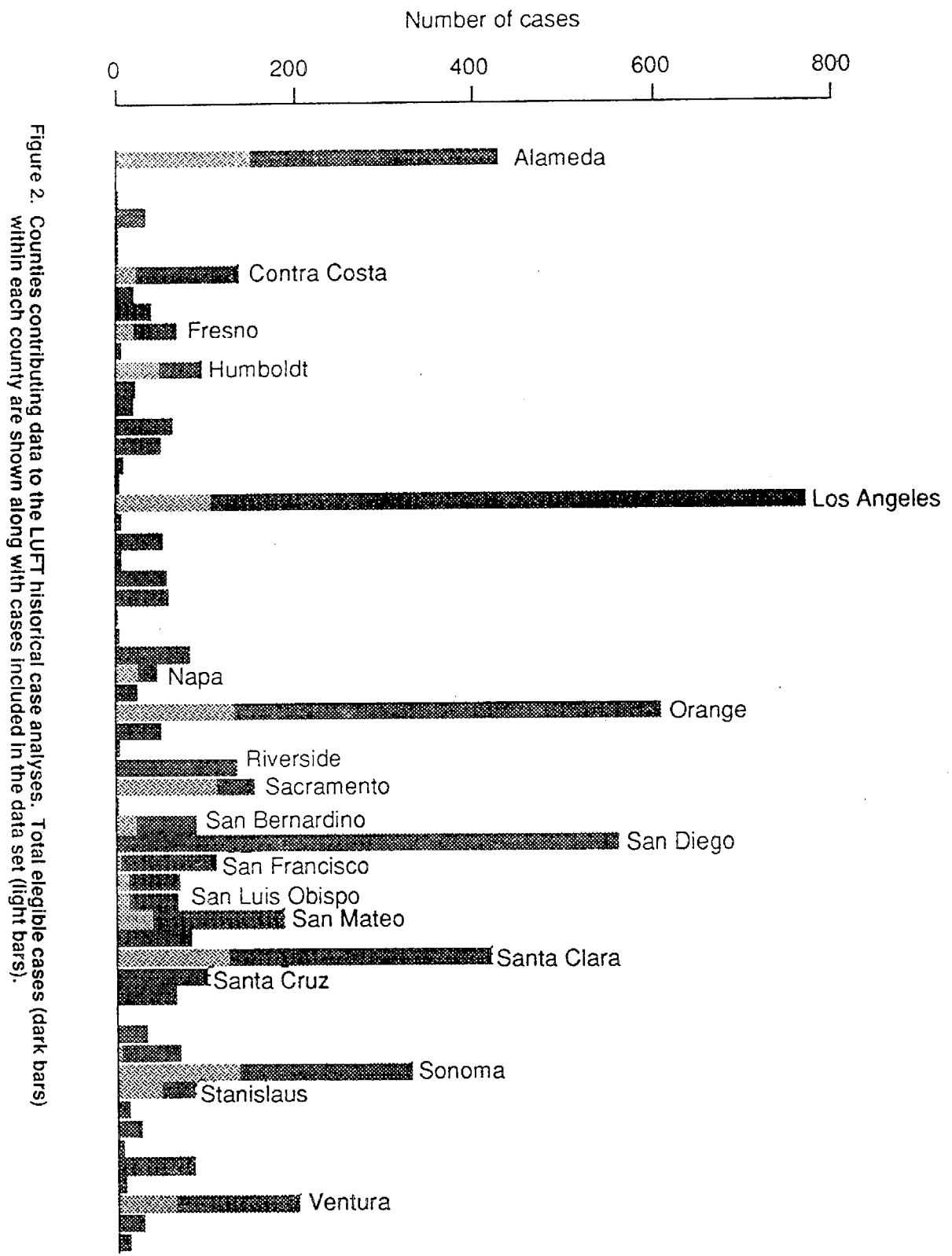


Figure 1. Uses of leaking underground fuel tank (LUFT) case data to support risk and resource management decision-making.



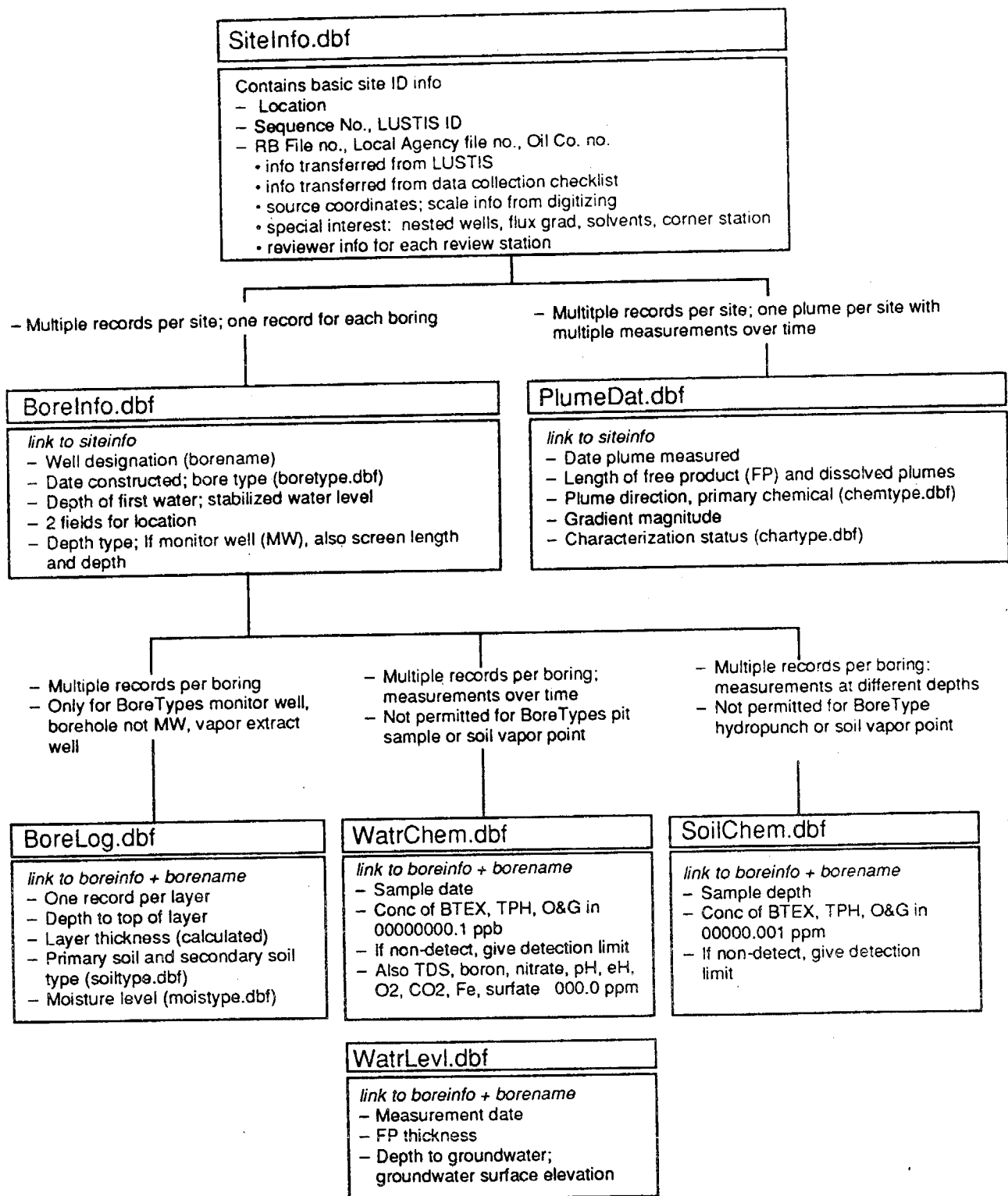


Figure 3. LUFT historical case analysis database structure.

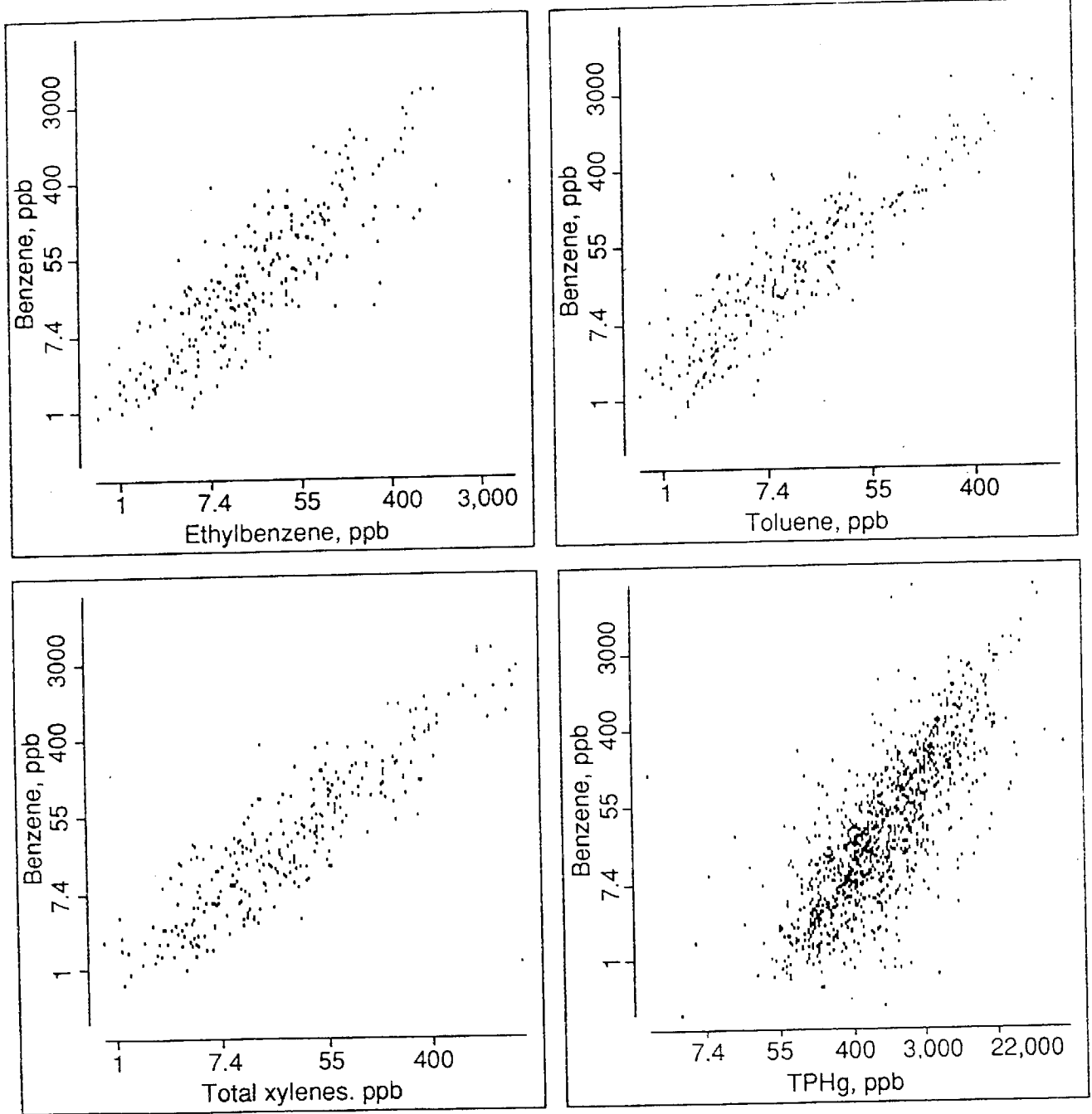


Figure 4. Scatter plots of site average benzene groundwater concentrations vs ethylbenzene, toluene, total xylenes, and total petroleum hydrocarbons (gasoline) (TPHg) concentrations.

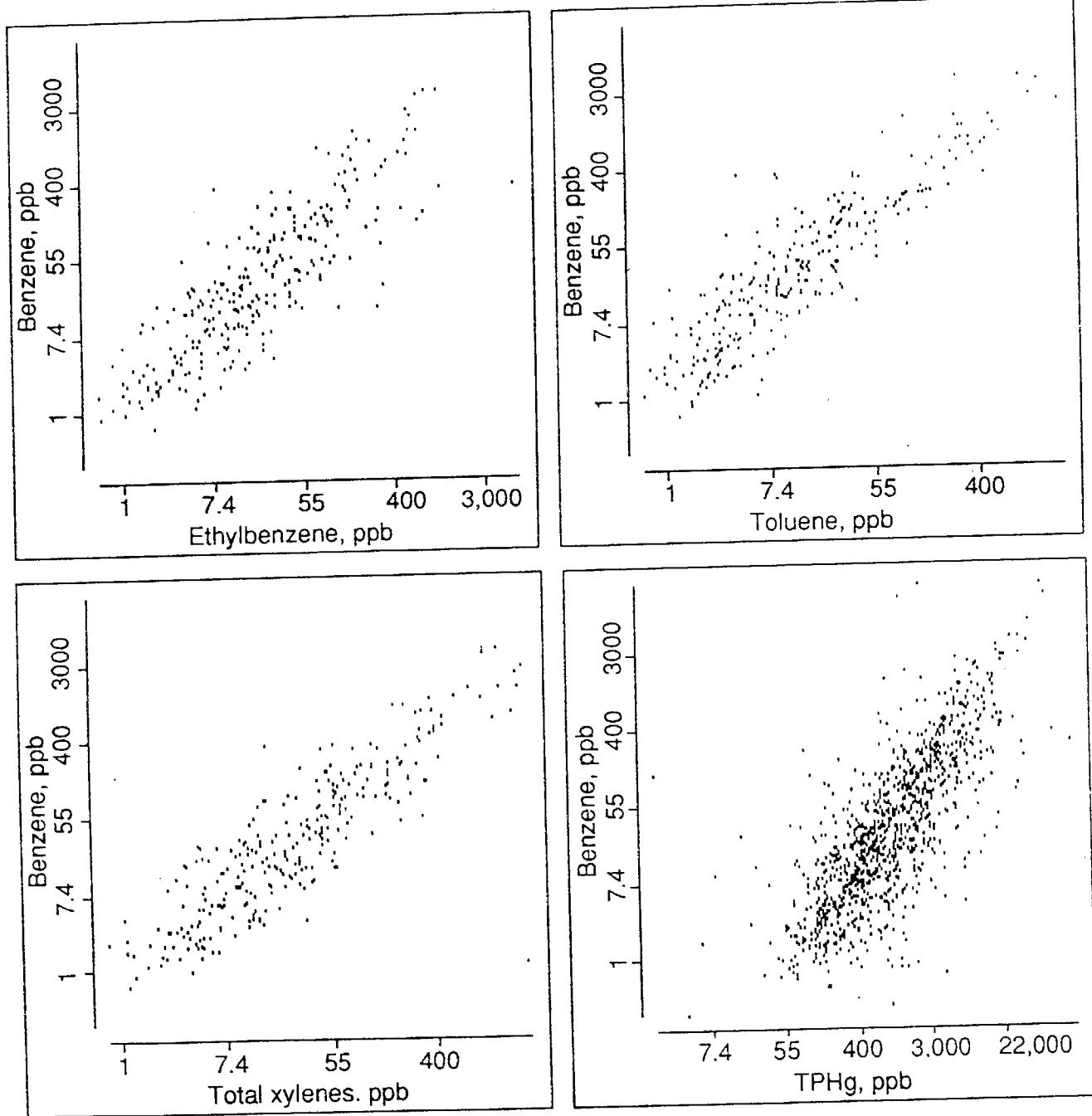


Figure 4. Scatter plots of site average benzene groundwater concentrations vs ethylbenzene, toluene, total xylenes, and total petroleum hydrocarbons (gasoline) (TPHg) concentrations.

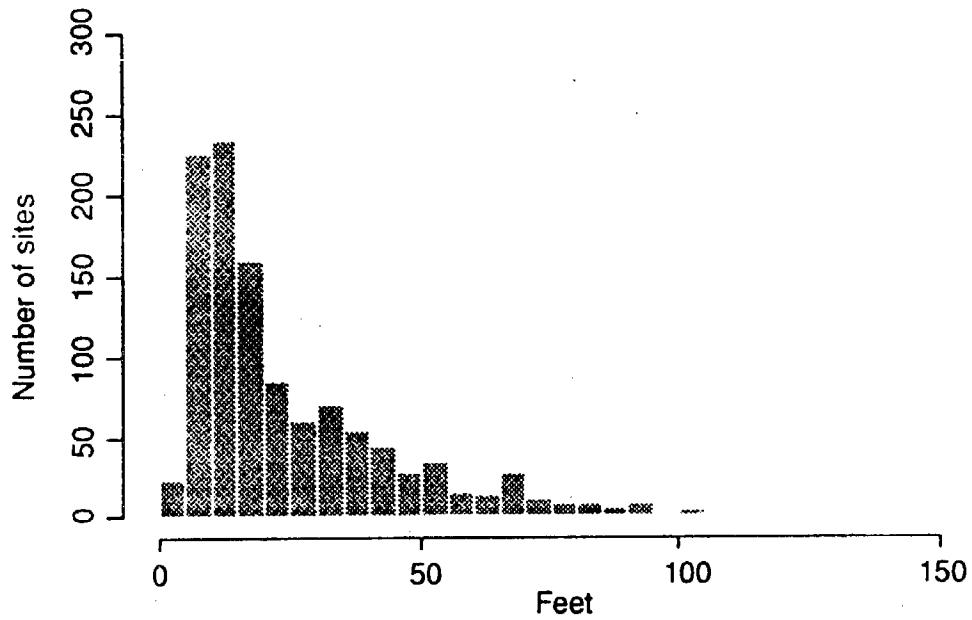


Figure 5. Site average maximum depth to groundwater.

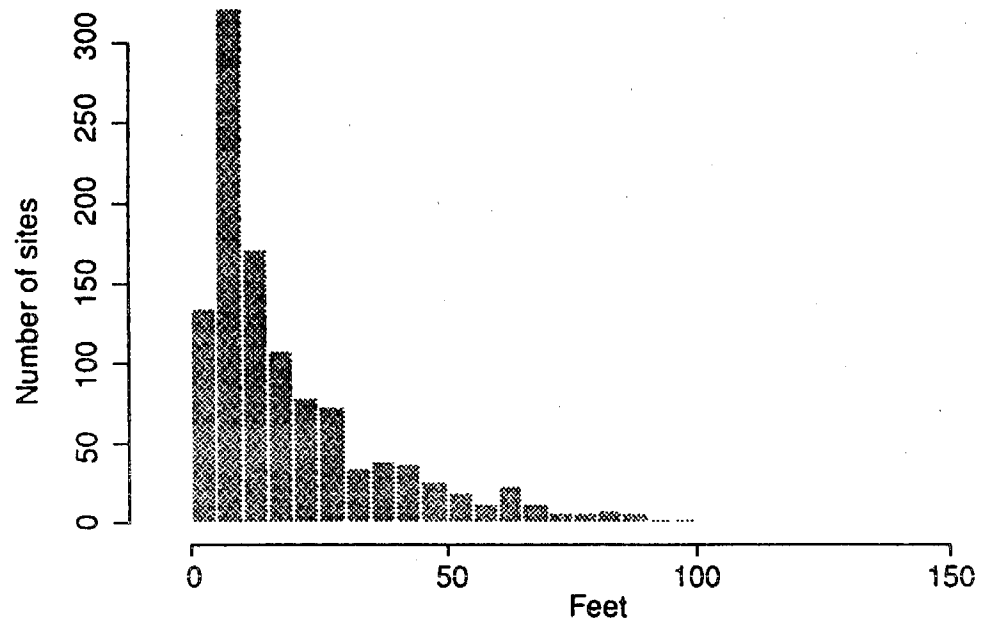
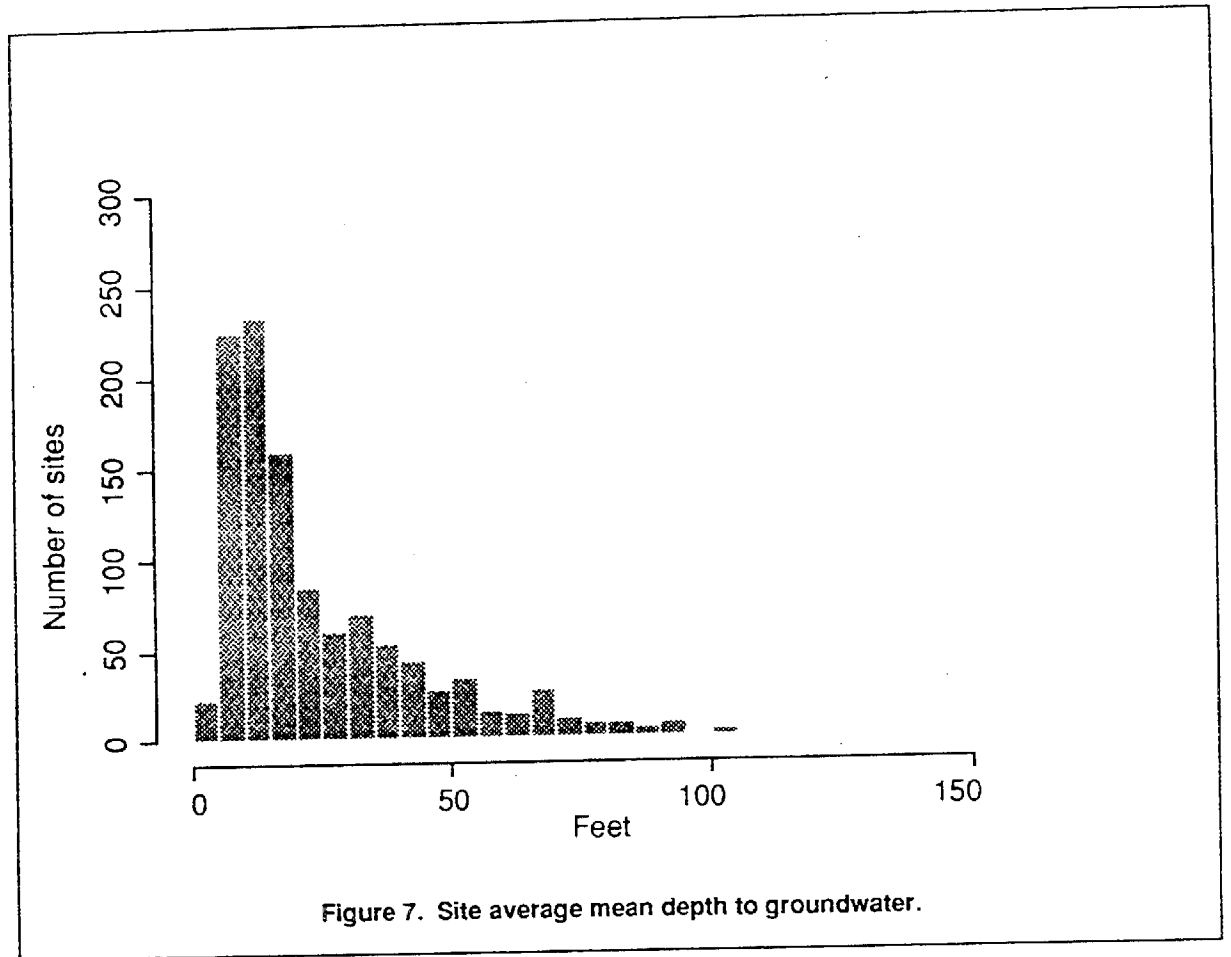
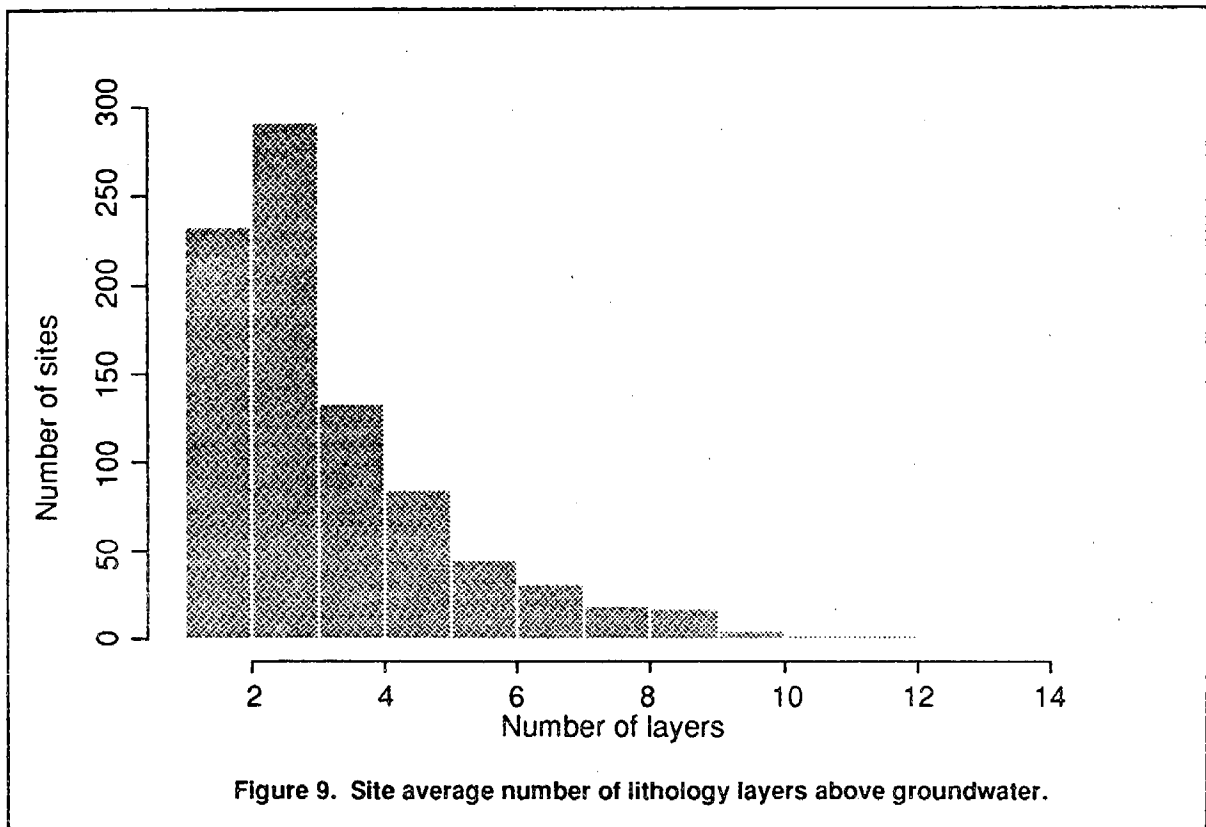
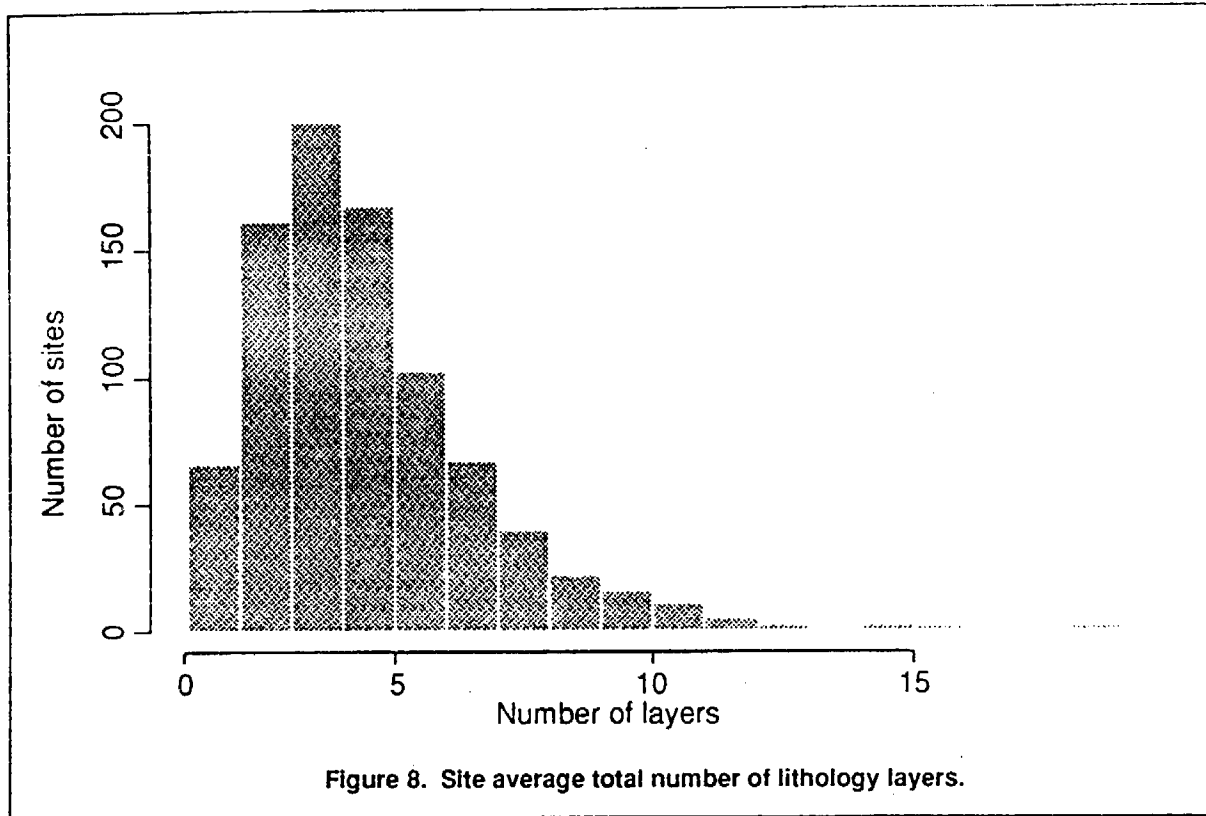


Figure 6. Site average minimum depth to groundwater.





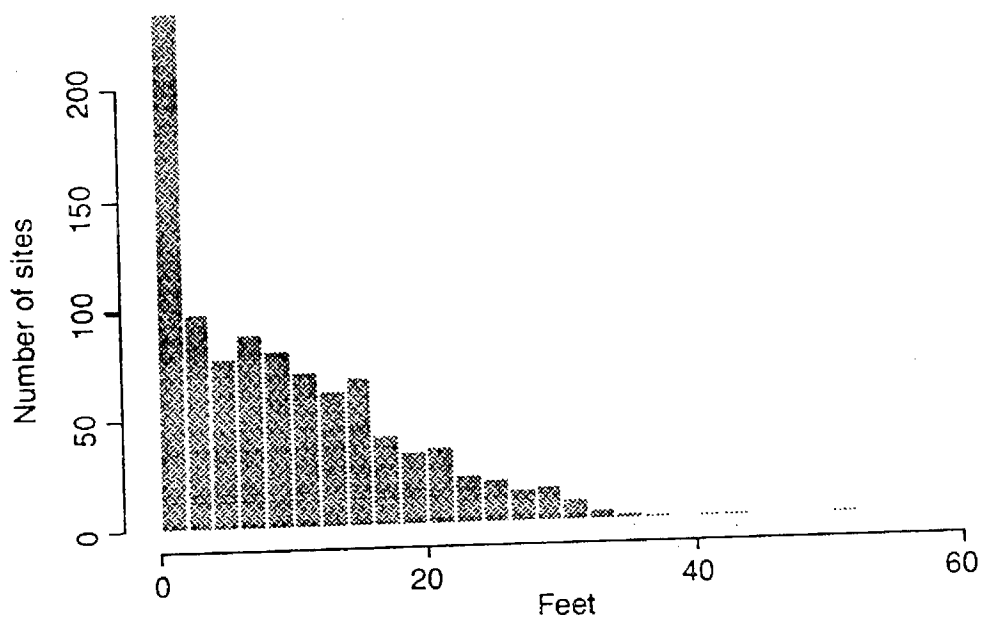


Figure 10. Site average total clay layer thickness.

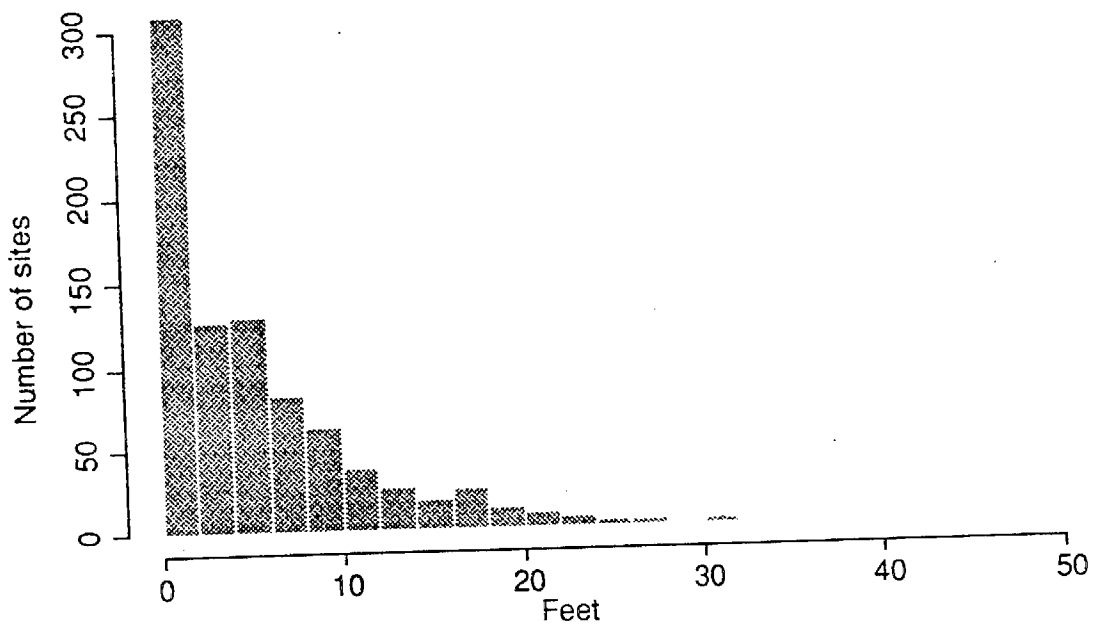


Figure 11. Site average total clay layer thickness above mean groundwater depth.

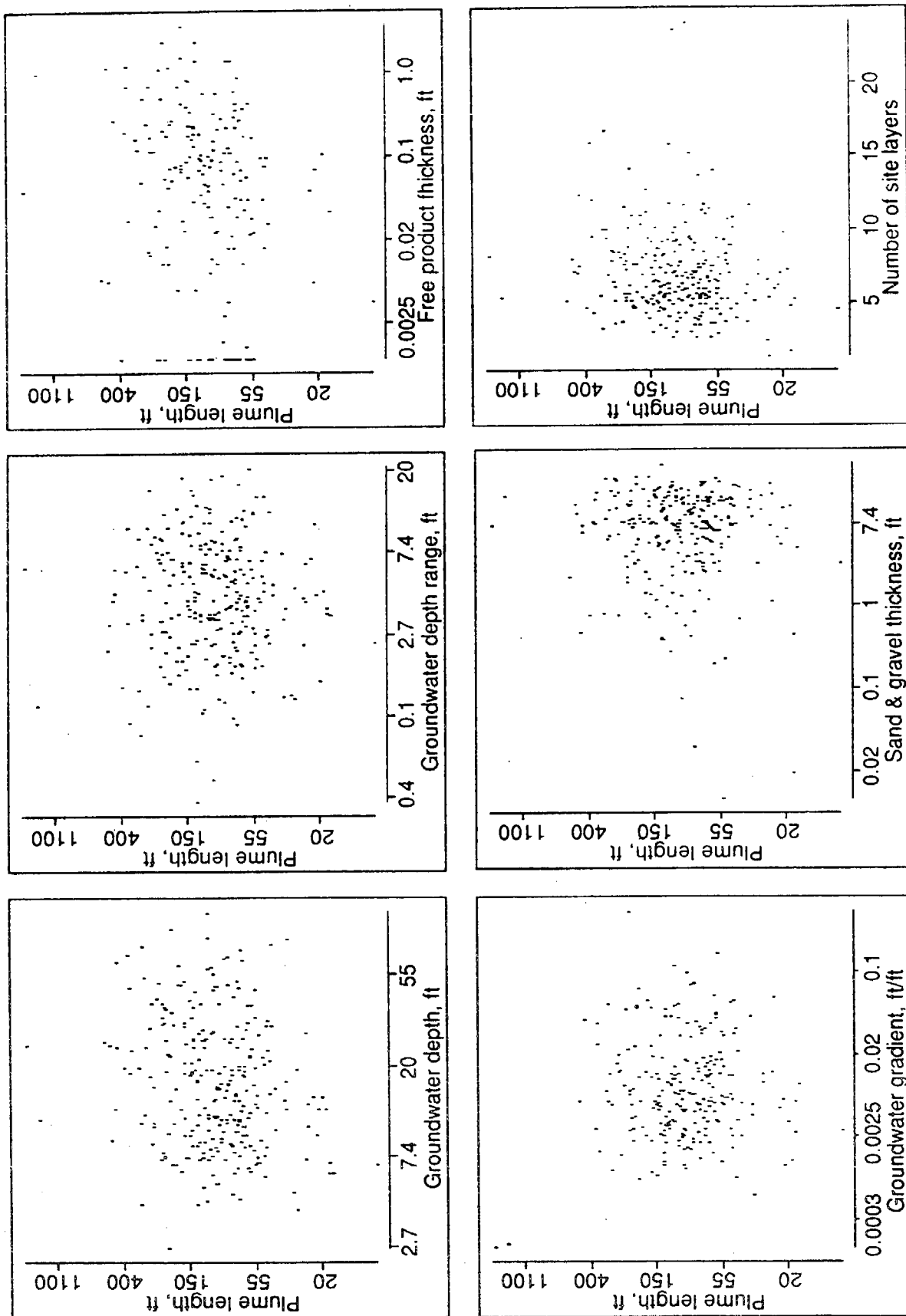


Figure 12. Error function model estimated average site plume lengths plotted against site average hydrogeologic characteristics.

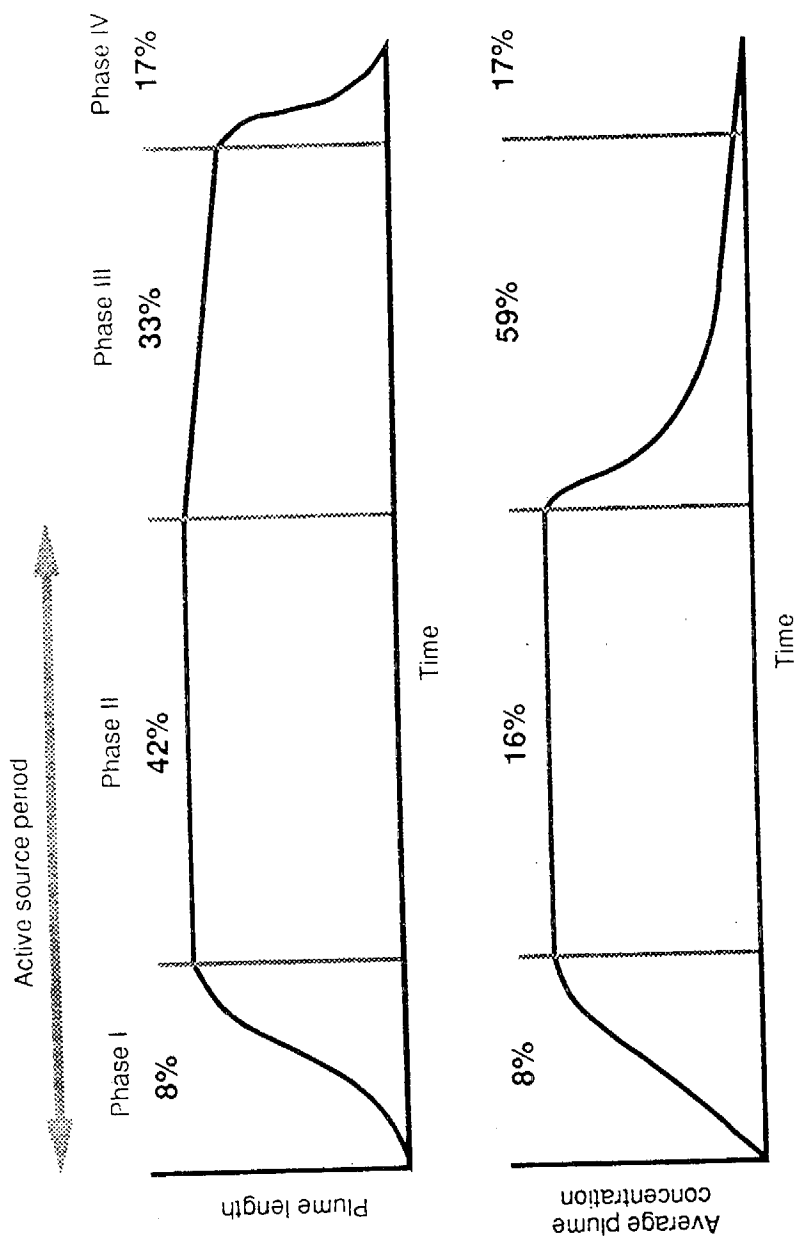


Figure 13. Hypothetical changes in plume average concentration and length during the life history of fuel hydrocarbons dissolved groundwater. The percentage of well characterized site ($n = 271$) that fall into each plume life history phase is also shown.

Appendix A

Degradation of FHCs Dissolved in Groundwater

Conceptual Model of the Fate and Transport of Fuel Hydrocarbons Released from a Leaking Underground Fuel Tank

The mechanisms by which spilled or leaked FHCs migrate in the subsurface at a site must be understood if effective investigative and remedial measures are to be implemented. Once liquid FHCs are released into the subsurface, they percolate through the unsaturated zone soil pore spaces, at first under the force of gravity. The lithologic heterogeneity, moisture content, and permeability of the soils determine the amount of liquid retained in the soil and the extent of the lateral spreading of liquid and gaseous hydrocarbons. As liquid- and gaseous-phase FHCs move through the unsaturated zone, they will follow the path of least resistance. When dense, low permeability layers are encountered, the bulk FHC liquid flowing under the force of gravity will tend to spread (Cole, 1994). A portion of the FHC mass will sorb onto soil particulates (Karickhoff *et al.*, 1979) or simply lodge in pore throat necks and dead-end pore spaces (Hunt *et al.*, 1988; Ahmed, 1989). The amount of FHC sorbed onto soil particulates is dependent on the amount of organic material and type of minerals present in the soil matrix (Karickhoff *et al.*, 1979).

The more soluble components of the FHC will tend to dissolve into the vadose zone water and can continue to migrate downward, or laterally, along with percolating recharge waters. When the dissolved aqueous phase is flowing under unsaturated conditions, coarse-textured dry layers with relatively large pore spaces act as barriers to aqueous FHC migration. Components of the FHCs with higher vapor pressure will volatilize and migrate in the vapor phase through air-filled pore spaces (Silka, 1986). Subsurface strata with high moisture content act as barriers to vapor migration.

Vapor diffusion is typically the dominant mechanism governing movement of FHC vapors in the subsurface. Rates of diffusion in the subsurface are much slower than those in free air space and influenced by the tortuosity of connected pore space channels. This tortuosity is influenced by and can be estimated by overall porosity and the volumetric air and water saturation percentages.

The amount of FHC volatilizing into pore spaces is influenced by the amount of water also present in the pore spaces and changes in barometric pressure, ground surface temperature fluctuations, and fluctuations in groundwater surface elevation, which force the air in the subsurface to move. Volatile FHC components in the soil pore spaces migrate away from the pure liquid and aqueous FHC trapped in the unsaturated zone (Falta *et al.*, 1989; Jury *et al.*, 1990). The lighter, more volatile chemicals, such as benzene, spread more rapidly than less volatile compounds, such as naphthalene.

Under the appropriate conditions, gas phase advection may dominate the transport of volatile compounds that originate from a bulk hydrocarbon liquid. This occurs mostly in soils with high permeability (Falta *et al.*, 1989). Advection driven by the density of the soil gas causes soil vapors with densities greater than air, such as FHCs, to have a tendency to move downward. The magnitude of density-driven flows is a function of the saturated vapor pressure of the organic liquid, the gas-phase permeability, and the gas-phase retardation coefficient. Benzene density-driven flow may occur, whereas for toluene, ethylbenzene, xylenes, naphthalene, and phenols, this is less likely (Falta *et al.*, 1989).

In addition to spreading horizontally and vertically as they migrate downwards to the water table, FHCs have a strong propensity to travel along conduits and pathways for lateral migration. Rock fractures, sand and gravel lenses, zones of high water content, indurated layers, and clay layers are natural structures that can control FHC movement. Manmade structures such as gravel backfill around subsurface utility lines, water and sewer lines, concrete and asphalt surfaces, septic leach lines, dry wells, and agricultural drains also commonly control FHC migration. Vapors follow these pathways and may lead to the discovery of the spill when they reach residences or businesses.

As the liquid or aqueous FHC continues to migrate downward, it reaches the capillary fringe of the water table. This is a zone where the soil pore spaces are mostly filled with water due to the tendency of water to be drawn up into the soil. Capillary fringe water is analogous to water drawn, or wicked up, into a paper towel dipped into water. The thickness of the capillary fringe is directly related to the size of pores as dictated by the lithology at a site. The thickness of the capillary fringe is typically greatest in fine-textured silty and clayey soils with small pore sizes and least in coarse-textured sand with relatively large pore sizes. As the term would indicate, the top of the capillary fringe is difficult to conclusively identify and changes with groundwater depth fluctuations. Because of a phenomenon known as hysteresis, the capillary fringe is generally thicker in declining water table conditions than it is during rising water table conditions. It is within the capillary fringe that the FHC becomes dissolved into the groundwater. Once bulk FHC reaches the capillary fringe of the water table, it is distributed through lateral spreading and becomes relatively immobile. Bulk FHC liquids must build up sufficient "head" to overcome the surface tension of capillary fringe water before they penetrate and come in contact with the underlying phreatic water.

As the groundwater flows, the dissolved FHCs generally move with the groundwater as a plume. As the plume moves, it spreads and, as in the unsaturated zone, part of the FHC mass sorbs onto soil particulates; part also is lost through volatilization into the soil pore spaces above the water table.

The sorption of the dissolved FHCs onto the soil particulates retards the movement of the plume relative to the groundwater flow. As long as there is continuing mass input from an active FHC source, the plume length will continue to grow until a point of stability is reached. This may be a point of pseudo-stability where the plume surface area expansion is large enough that the rate of spreading is very slow and difficult to detect. The point of plume pseudo-stability in the absence of passive biodegradation can be calculated (Buscheck *et al.*, 1993; McAllister and Chiang, 1994).

It is now known that when plume lengths are measured in the field, plume length stability is often reached at a distance from the source much less than what would be calculated.

Groundwater scientists recognize that a major factor responsible for the shorter stable plume lengths is the action of indigenous soil microorganisms that are using FHCs as a food source and removing FHC mass from the plume (Barker *et al.*, 1987; Rifai *et al.*, 1988; Chiang *et al.*, 1989; Cozzarelli *et al.*, 1990; Baedeker *et al.*, 1992; Baedeker *et al.*, 1993; Bennett *et al.*, 1993; Eganhouse *et al.*, 1993; Reinhard, 1993; Salanitro, 1993; Cozzarelli *et al.*, 1994; NRC, 1994; Borden *et al.*, 1995; McNab and Narasimhan, 1995).

Passive Bioremediation Processes

As oxygen-rich water flows through a FHC source area, FHCs become dissolved in the groundwater and are transported downgradient. Ubiquitous microbial populations in the soil are stimulated and begin degrading the FHC to organic acid intermediates, and finally carbon dioxide and water. The microbes preferentially use oxygen as an electron acceptor, but switch to other electron acceptors such as NO_3^- , Fe^{+2} , Mn^{+2} , and SO_4^{2-} , until methanogenic conditions ultimately develop (Haag *et al.*, 1991; Cozzarelli and Baedeker, 1992; Salanitro *et al.*, 1993; Beller and Reinhard, 1995). This process results in a large core area of the plume in which, oxygen, pH and redox measurements are low and inorganic ion measurements of NO_3^- , Fe^{+2} , Mn^{+2} , and SO_4^{2-} may be expected to be reduced. Around the margins of the plume is a transition zone in which oxygen becomes increasingly more available and aerobic microbial degradation of FHCs proceeds. Typically, biodegradation of FHCs proceeds more rapidly under aerobic conditions, but a bulk of the FHC mass is degraded more slowly because the anaerobic core of the plume is much larger in surface area than the aerobic plume margins.

The ability of microbes to degrade FHCs will be limited by the availability of electron acceptors (Bouwer and McCarty, 1984; Vogel *et al.*, 1987), but Air Force studies indicate that in many geochemical environments, the availability of electron acceptors is not limiting, and there is usually an excess potential microbial FHC biodegradation (Wilson *et al.*, 1994). Because of this excess biodegradation capacity, a FHC plume may be expected to remain stable in length and mass, in spite of the presence of an active source that may be continually dissolving new FHC mass into the plume.

Appendix B

Implementation of Plume Models

Plume Length Calculations

The following sections describe the methods used to estimate the size of dissolved benzene groundwater plumes for the sites in the LUFT historical database. Impacts to the saturated zone are assessed by estimating the spatial extent, in two dimensions, of the contamination present in groundwater at each of the sites. The approach adopted was to fit the observed spatial distributions of the contaminant concentrations to simple mathematical plume models using standard statistical methods. Estimates of benzene plume dimensions at each site were then computed from the fitted model parameters based on characteristic plume geometries.

Principal Plume Model Assumptions

Because most sites in the LUFT database have monitoring wells completed at only one geologic horizon, most of the analytical data is 2-D. The models used to estimate plume dimensions assume that plumes have a center, or source area, that can be roughly estimated by the spatial center of mass of the contaminant distribution. The models also assume that contaminant concentrations will generally decline with distance from the center of the plume in all directions. Hence, the essential feature of the developed plume model algorithms is that they predict concentration isocontours that are represented by continuous, closed curves in 2-D space. Observed contaminant spatial distributions that appear to be essentially flat or planar in character cannot be well approximated by the mathematics of the plume models, and they may not be able to be fitted at all.

Overview of Plume Models

The developed plume models attempt to describe the observed monitoring well concentrations, measured at each of the LUFT sites during a seven-day window in time, as functions of the monitoring well coordinates:

$$C(x,y) = f(x,y;\alpha,\beta,\gamma,\delta,\dots).$$

Here, $C(x,y)$ represents the analyte concentration observed at the well located at geographic position (x,y) , and $\alpha,\beta,\gamma,\delta$, etc., represent parameters of the model that need to be estimated for each set of temporal observations. The models can be viewed as having a characteristic shape that, for each model, obtains its specific attributes from a particular set of parameters. Typically, these parameters are related to (1) the peak levels of contaminant concentrations measured at the site, and (2) the amount of lateral spreading (dispersion) that has occurred at the site.

Once a particular model has been fitted, the lateral extent of contamination can generally be estimated from the geometry of the fitted model. That is, for some level of contamination (e.g.,

10 ppb benzene), the estimated length and width of the contaminant plume can be computed as some known function of the fitted model parameters:

$$l = g(\alpha, \beta, \gamma, \delta, \dots)$$

$$w = h(\alpha, \beta, \gamma, \delta, \dots),$$

where l and w represent the estimated length and width, respectively, of the contaminant plume for the site at a particular point in time. Under the linear model, for example, predicted concentration isocontours take the form of ellipses, and the estimated plume lengths and plume widths are defined to be the lengths of the semi-major and semi-minor axes of these ellipses, respectively.

Hence, the models produce time series estimates of plume length and width for each site in the database. Typically, these time series values are summarized to yield time-average plume lengths and widths, and their variances, for each of the sites.

Model Fitting Considerations

In general, when fitting data to a given functional form, there must be more data points than parameters in the model. When fitting a linear model by linear regression (or, equivalently, maximum likelihood estimation), it is theoretically assured that a perfect fit will be obtained if we have exactly as many data points as there are model parameters. Whenever there are more observations than model parameters, the additional observations can be used to investigate the "goodness of fit" of the model, or, equivalently, the amount of "error" associated with the model fit. The number of observations beyond the number of model parameters is commonly referred to as the number of "error degrees of freedom." The more error degrees of freedom for any given model, the better we are able to assess the model's performance. Accordingly, a perfect fit (in the case of a linear model) has zero error degrees of freedom, and the goodness of fit of the model cannot usually be assessed.

Implementation of Plume Models

Two principal models have been developed to investigate plume evolution using the LUFT historical database data. Both of these models in their full form have four parameters, and, thus, they require a minimum of five observations to obtain an estimate of error along with the model parameters. The first model, which is based on an exponential form, can be expressed in linear form, and, therefore, simple linear regression, also known as least-squares fitting, can be used to estimate the model parameters. The second model, which is based on error functions, cannot be linearized, and its parameters must be estimated by using iterative procedures.

Despite the inherent differences in the models and the methods used to fit them, the fitting procedures share certain essential features. From the outset, it was recognized that many of the LUFT database sites would have a small number of installed monitoring wells and would, therefore, only provide a few data points for model fitting. Moreover, the fitted plume orientation was subject to considerable error and was particularly sensitive to the placement of the observation wells. Hence, estimating plume orientations for sites with few data points was of questionable merit. Based on an evaluation of the number of available sites with sufficient observation points, it was decided that a minimum of six observation locations would be required to yield an accurate assessment of plume orientation under either model. Because both plume

models have four parameters, this requirement would ensure two error degrees of freedom for evaluating the model fits.

During the use of both models, the water chemistry data are preprocessed in the following sequence of stages:

- Data for each site are arranged in chronological order.
- All observed "non-detects" are converted to a value of one-half of the detection limit of the indicator analyte (non-detects are considered observational data and are counted in the number of error degrees of freedom).
- All well observations that indicate the presence of free product in lieu of an analytical concentration are assigned an estimated benzene concentration. This estimated benzene concentration was based on frequency of occurrence of observed free product in the monitor well. If free product was always observed in the monitor well, then the benzene groundwater concentration was estimated to be the maximum benzene concentration observed at the site. If free product was observed during only part of the monitor well's observation periods, then the benzene groundwater concentration was estimated to be the maximum benzene concentration measured in that monitor well.
- Data samples are assigned to "sampling episodes" on the basis of the sample collection date. Sampling episodes consist of up to seven consecutive days of samples taken at an individual site, and are identified by the date of the first day in the interval.
- Data samples that represent "no information available" are eliminated from the data in the sampling episodes (non-detects are retained as real data in this step). The number of remaining data samples available in each sampling episode is stored.
- If all the data samples available in a particular sampling episode have the same value (e.g., all non-detect), then the sampling episode is ignored (no model is fitted—no plume lengths or masses are returned).
- If the number of data samples available in a particular sampling episode is smaller than the number of parameters in the plume model plus one, then no model can be fitted, and all the data for the sampling episode are ignored.
- The analytical center of mass (\bar{x} , \bar{y}) is computed for each sampling episode, and the well coordinate system for the site is translated to this center, i.e., the current center of mass of the contaminant system becomes the new geographic origin for purposes of fitting the plume model to sampling episode data; the center of mass of the contaminant system becomes the new geographic origin for purposes of fitting the plume model to sampling episode data; and the center of mass of the system will thus coincide with the center of the fitted plume.
- If the nonlinear error function model is to be fitted, then the orientation of the principal mass moments of inertia of the sampling episode data are computed, and the well coordinate system is rotated so that the new x-axis coincides with the direction of the smaller mass moment of inertia. When the error function plume model is fitted to the data in the new reference frame, the orientation of the resulting plume is effectively constrained to coincide with one of the principal mass moments of inertia.

General Behavior of Plume Algorithms

Theoretically, the exponential (linear) plume model fitting algorithm should always be able to return a result (unless all observations are the same number) because the fitting is done via linear least squares, i.e., a unique solution should exist. The error function (nonlinear) plume model fitting procedure, on the other hand, is based on the iterative Levenberg–Marquardt (L–M) algorithm, which attempts to determine optimal model parameters by minimizing the residual sum-of-squares for each set of data observations. The L–M procedure requires an initial guess for the parameter values, and is not generally guaranteed to converge to a consistent solution. An objective function with multiple modes, for example, may have several relative minima. Moreover, the L–M procedure can be very sensitive to the initial starting point, to the degree that one initial guess may yield rapid convergence to a reasonable solution, while a nearby point may lead the algorithm off into an infeasible solution domain and ultimately to a numerical overflow or underflow situation, i.e., a program crash.

For the groundwater contamination data in the LUFT database, the exponential model was found to be very sensitive to the occurrence of low concentration values at large distances from the contaminant center of mass of the monitoring well system. This sensitivity is due to the relatively rigid shape described by the exponential model. The occurrence of small concentrations at large distances from the “source” have the effect of “stretching out” the exponential decay curve, thus resulting in relatively large predicted plume lengths. Because a large proportion of the outlying observations at the database sites represents “non-detects” rather than actual measured concentration values, long plume lengths returned by the exponential model were scrutinized carefully. Overall, the exponential model algorithm yields a substantial amount of site-by-site variability in predicted plume lengths and masses. On the other hand, the linear model does provide a conservative measure, from a risk assessment perspective, of the lateral extent of contamination.

Due to the great flexibility in the shape of the error function (nonlinear) plume model, the sensitivity to small outlying concentrations is greatly reduced. The error function model can allow concentration levels to be essentially flat in the source area and yet have them drop off very quickly to non-detect levels within a relatively small distance from the source area. In a large percentage of the cases, this model fits the observational data better than the exponential model, as evidenced by the higher R^2 values (coefficients of multiple correlation) and lower mean square errors. Consequently, the error function model frequently returns substantially smaller predicted plume lengths than the exponential model. In many cases, however, the error function model fails to obtain a reasonable fit to the observed data, perhaps due to the lack of a good starting point, and it therefore exhibits more site-by-site variability in its predictions than that produced by the exponential model. The error function program is particularly susceptible to instances in which a large percentage of the observed concentration values are of the same order of magnitude, e.g., five non-detects and one low-level hit, or five free products and one non-detect; here, the model is likely to either produce astronomical plume lengths or simply crash.

Appendix C

The Exponential (Linear) Plume Model

The 2-D exponential plume model is loosely based on the Baetsle instantaneous point source model (cf. Freeze and Cherry, 1979). The fundamental form of the model is

$$C(x, y; C_0, D_x, D_{xy}, D_y) = C_0 \exp\left[-(D_x x^2 + D_{xy} xy + D_y y^2)\right], \quad (C-1)$$

where C_0 , D_x , D_{xy} , and D_y are the model parameters to be fitted, and

$$C(x, y; A, D_x, D_{xy}, D_y) = \text{analyte concentration observed at well at } (x, y) \{M / L^3\} \quad (C-2)$$

C_0 = overall site contamination level $\{M / L^3\}$

D_x = parameter for dispersion in the x - direction $\{L^{-2}\}$

D_{xy} = parameter for dispersion in the xy - direction $\{L^{-2}\}$

D_y = parameter for dispersion in the y - direction $\{L^{-2}\}$

x = geographic x - coordinate measured relative to center of mass at site $\{L\}$

y = geographic y - coordinate measured relative to center of mass at site $\{L\}$.

This equation can be fitted to observed monitoring well concentration data on a site-by-site basis for every sampling episode in the site's history. Observe that the D_{xy} term effectively controls the orientation of the plume in 2-D space.

The form above can be linearized by taking logarithms to yield

$$\log[C(x, y; C_0, D_x, D_{xy}, D_y)] = \log(C_0) - D_x x^2 - D_{xy} xy - D_y y^2 \quad (C-3)$$

or, alternately,

$$D_x x^2 + D_{xy} xy + D_y y^2 = \log(C_0) - \log[C(x, y; C_0, D_x, D_{xy}, D_y)]. \quad (C-4)$$

The equation above is known as a quadratic form, and its graphical representation is referred to as a conic section. This equation predicts the shape of the contaminant isocontour (at the level of C) for the model represented by Eq. C-1. In fact, the equation above described an ellipse whenever the condition

$$D_{xy}^2 - 4D_x D_y < 0 \quad (C-5)$$

is satisfied, and it describes a hyperbola under the condition

$$D_{xy}^2 - 4D_x D_y > 0. \quad (C-6)$$

Observe here that if D_x and D_y are equal, then the D_{xy} term is superfluous, since the ellipse reduces to a circle, which has no preferred orientation.

To make the above model conform to our ideal plume model, we need to eliminate the hyperbola condition above and only accept plumes that have closed isocontours (ellipses). This can be done by eliminating the D_{xy} term from the full model above whenever it returns a hyperbolic form, and fitting a simpler model where $D_x = D_y \equiv D_r$ in its place. For this "reduced" model, concentration isocontours always appear as circles. The reduced exponential model then takes the form

$$C(x, y; C_0, D_r) = C_0 \exp[-D_r(x^2 + y^2)], \quad (C-7)$$

which has the simple linear representation

$$x^2 + y^2 = \{\log(C_0) - \log[C(x, y; C_0, D_r)]\} / D_r, \quad (C-8)$$

(the equation for a circle).

For this simplified model, an obvious choice for the characteristic plume length (associated with a contaminant concentration level of C^* , say) would simply be the radius of the circle

$$r = \sqrt{x^2 + y^2} = \sqrt{[\log(C_0) - \log(C^*)] / D_r}. \quad (C-9)$$

Similarly, the corresponding metrics for the characteristic length and width of an elliptical plume from the full model (again, associated with a contaminant concentration level of C^*) would be the lengths of the semi-major and semi-minor axes, respectively, of the predicted isocontour ellipse:

$$M = \frac{2\pi C_0}{\sqrt{4D_x D_y - D_{xy}^2}}. \quad (C-10)$$

where

$$\begin{aligned} \sigma_1 &= \frac{2D_x[D_{xy}^2 + (D_y - D_x)^2] + [2D_x(D_y - D_x) - D_{xy}^2]\sqrt{(D_y - D_x)^2 + D_{xy}^2}}{\left[(D_y - D_x) + \sqrt{(D_y - D_x)^2 + D_{xy}^2}\right]^2 + D_{xy}^2} \\ \sigma_2 &= \frac{2D_y[D_{xy}^2 + (D_y - D_x)^2] + [2D_y(D_y - D_x) + D_{xy}^2]\sqrt{(D_y - D_x)^2 + D_{xy}^2}}{\left[(D_y - D_x) + \sqrt{(D_y - D_x)^2 + D_{xy}^2}\right]^2 + D_{xy}^2} \end{aligned} \quad (C-11)$$

The foregoing equations are obtained by identifying the eigenvalues of the quadratic form in Eq. C-1 and constructing the orthogonal transformation matrix, which diagonalizes the quadratic form. Notice that when $D_{xy} = 0$, the ellipse is in standard position (aligned with the x- and y-axes), and the parameters above reduce to

$$\begin{aligned} \sigma_1 &= D_x \\ \sigma_2 &= D_y \end{aligned} \quad (C-12)$$

In this particular instance, the plume length and width estimates are simple

$$\begin{aligned}
 l &= \max \left\{ \sqrt{[\log(C_o) - \log(C^*)] / D_x}, \sqrt{[\log(C_o) - \log(C^*)] / D_y} \right\} \\
 w &= \min \left\{ \sqrt{[\log(C_o) - \log(C^*)] / D_x}, \sqrt{[\log(C_o) - \log(C^*)] / D_y} \right\},
 \end{aligned}
 \tag{C-13}$$

as must be the case.

Observe that the plume lengths and widths for both the full and reduced models are nonlinear functions of the model parameters. Since most model fitting procedures also estimate the uncertainties associated with the fitted model parameters, we have some information available regarding the variability in the predicted plume lengths. However, because of the nonlinear dependence of the plume lengths on the model parameters, the estimated variances of the estimated plume lengths and widths cannot be expressed in closed analytical form. These variances must be estimated by numerical methods.

Appendix D

The Error Function (Nonlinear) Plume Model

The 2-D error function plume model is loosely based on the Domenico–Robbins continuous line source model (Domenico and Robbins, 1985). The fundamental form of the model is

$$C(x,y;C_o,D_x,D_y,L_s) = \frac{M_o}{16L_s^2} \left\{ \text{erf}[D_x(x+L_s)] - \text{erf}[D_x(x-L_s)] \right\} \cdot \left\{ \text{erf}[D_y(y+L_s)] - \text{erf}[D_y(y-L_s)] \right\}, \quad (\text{D-1})$$

where M_o , D_x , D_y , and L_s are the model parameters to be fitted, and

$$C(x,y,A,D_x,D_y) = \text{analyte concentration observed at well at } (x,y) \{M/L^3\}$$

$$M_o = \text{total amount of contaminant mass per unit saturated thickness } \{M/L\}$$

$$D_x = \text{parameter for dispersion in the } x \text{ - direction } \{L^{-1}\}$$

$$D_y = \text{parameter for dispersion in the } y \text{ - direction } \{L^{-1}\}$$

$$L_s = \text{characteristic source dimension } \{L\}$$

$$x = \text{geographic } x \text{ - coordinate measured relative to center of mass at site } \{L\}$$

$$y = \text{geographic } y \text{ - coordinate measured relative to center of mass at site } \{L\}.$$

This model describes the (2-D) spatial contaminant distribution that could be expected to result from a continuous point source release in an anisotropic subsurface environment in the absence of a predominant groundwater flow direction. That is, the above model represents a contamination scenario in which molecular diffusion plays a prominent role in the transport of chemical constituents.

Equation D-1 can be fitted to observed monitoring well concentration data on a site-by-site basis for each sampling episode in a site's history. For the model above, the orientation of the plume must be specified before fitting the equation to the observed concentrations. The directions of the principal mass moments of inertia of the contaminant distribution, measured with reference to the center of mass of the system, can be used as a first-order estimate of the plume orientation. For this investigation, the mass moments of inertia of the contaminant distribution are estimated by

$$I_{xx} = \sum c_i y_i^2 \quad (\text{D-2a})$$

$$I_{yy} = \sum c_i x_i^2 \quad (\text{D-2b})$$

$$I_{xy} = \sum c_i x_i y_i, \quad (\text{D-2c})$$

where the sum is taken over the number of monitoring wells with observed concentrations $c(x,y)$. The principal mass moments of inertia are determined by finding the coordinate system rotation

for which $I_{x'y'} = 0$. The rotation angle for the required transformation can be expressed in terms of the moments above (Meriam, 1975),

$$\theta = \frac{1}{2} \tan^{-1} \left(\frac{-2I_{xy}}{I_{xx} - I_{yy}} \right) \quad (D-3)$$

and the magnitudes of the principal moments may then be obtained from

$$I_{x'x'}, I_{y'y'} = \frac{I_{xx} + I_{yy}}{2} \pm \sqrt{\left(\frac{I_{xx} - I_{yy}}{2} \right)^2 + I_{xy}^2} \quad (D-4)$$

Since the mass moments measure the amount of dispersion perpendicular to the reference axis, we identify the orientation of the long dimension of the plume with the axis of the smaller principal mass moment.

We recognize that the principal mass moment method does not reliably identify the optimal plume orientation, and it performs particularly poorly when the magnitudes of the principal mass moments are nearly the same.

Equation D-1 represents the contaminant distribution as a nonlinear function of the parameters. Since this equation cannot be represented in linear form, the observed contaminant concentration data must be fitted to the model using iterative numerical methods. For this procedure, we employ the Levenberg-Marquardt optimization procedure, which seeks the parameters that minimize the sum of squared residuals between the concentrations predicted by **Eq. D-1** and the actual observed concentration values. The Levenberg-Marquardt method (Draper and Smith, 1981; Press *et al.*, 1992) is a hybrid Taylor's series-steepest descent optimization procedure. The method is known to be robust for a wide variety of nonlinear problems, since it allows for the possibility of ill-conditioning. Seber and Wild (1989) provides a more technical description of the method and discusses the circumstances under which the procedure is known to perform poorly.

Once the optimal parameters of the model have been determined for a particular set of observations, the characteristic plume width and length (corresponding to a contaminant concentration level of C^* , say) may be estimated by solving the equations

$$C^* = \frac{M_o}{8L_s^2} \operatorname{erf}(D_x L_s) \left\{ \operatorname{erf}[D_y(y + L_s)] - \operatorname{erf}[D_y(y - L_s)] \right\} \quad (D-5)$$

and

$$C^* = \frac{M_o}{8L_s^2} \operatorname{erf}(D_y L_s) \left\{ \operatorname{erf}[D_x(x + L_s)] - \operatorname{erf}[D_x(x - L_s)] \right\} \quad (D-6)$$

for y and x respectively. The foregoing equations are derived from **Eq. D-1** by consecutively setting x and y , respectively, equal to zero. The equations above cannot be solved analytically; instead, the solutions may be obtained by numerically finding the roots, x and y , of the functions

$$g(y; C^*, D_x, D_y, L_s) = \operatorname{erf}[D_y(y + L_s)] - \operatorname{erf}[D_y(y - L_s)] - \frac{8C^* L_s^2}{M_o \operatorname{erf}(D_x L_s)} \quad (D-7a)$$

$$h(x; C^*, D_x, D_y, L_s) = \text{erf}[D_x(x + L_s)] - \text{erf}[D_x(x - L_s)] - \frac{8C^* L_s^2}{M_o \text{erf}(D_y L_s)}. \quad (\text{D-7b})$$

The larger of the two roots represents the characteristic length of the plume, while the other represents its characteristic width.

As in the case of the exponential plume model, the error function model can be reduced to a form that is symmetric in both coordinate directions. In this case, the model has the form

$$C(x, y; C_o, D_r, L_s) = \int \frac{M_o}{16L_s^2} \left\{ \text{erf}[D_r(x + L_s)] - \text{erf}[D_r(x - L_s)] \right\} \cdot \left\{ \text{erf}[D_r(y + L_s)] - \text{erf}[D_r(y - L_s)] \right\}, \quad (\text{D-8})$$

and the characteristic plume length and plume width are both represented by the root of the function

$$h(x; C^*, D_r, L_s) = \text{erf}[D_r(x + L_s)] - \text{erf}[D_r(x - L_s)] - \frac{8C^* L_s^2}{M_o \text{erf}(D_r L_s)}, \quad (\text{D-9})$$

where D_r is a coefficient for radial molecular dispersion $\{\text{L}^{-1}\}$.

Observe that the plume lengths and widths for both the full and reduced models are nonlinear functions of the model parameters. Since most model fitting procedures also estimate the uncertainties associated with the fitted model parameters, we have some information available regarding the variability in the predicted plume lengths. However, because of the nonlinear dependence of the plume lengths on the model parameters, the estimated variances of the estimated plume lengths and widths cannot be expressed in closed analytical form. These variances must be estimated by numerical methods.

Appendix E

Emerging Technologies To Support a Revised LUFT Cleanup Process

Characterization technologies are critical to a revised LUFT cleanup approach. To support a tiered risk-based decision-making process, emphasis should be placed on methods to better define the spatial distribution of hydrogeologic conditions that affect the fate of fuel hydrocarbons (FHCs). If the plume stability and mass reduction resulting from intrinsic bioremediation is to be relied upon, then enhanced characterization and monitoring will be required. To manage and implement passive intrinsic remediation at a site, a trade-off will be to enhance the site characterization rather than incur the cost of an extended actively engineered remediation.

This enhanced characterization need not be more expensive than more traditional methods. In many situations, a greater number of sampling points with a screening level data quality objective is preferable to a few data points with high analytical precision.

Soil gas surveys can be used as a screening tool during an initial phase of an FHC source characterization/monitoring program when the FHC, e.g., gasoline, has a significant volatile component. Soil gas investigations typically involve either a constant-depth horizontal-distribution soil gas survey and/or a horizontal and vertical soil gas survey in an attempt to quickly track and locate the mass of hydrocarbon *in situ*. In addition, soil gas surveys can, in appropriate cases, be used to track and infer the presence of free-phase and dissolved-phase contamination. Soil gas surveys tend to be effective if vertical migration of gases is not constrained by the presence of fine-grained or high-water-content materials or indurated strata. Soil gas sampling points can be completed and left in place for access at a future date to assess the progress of the remediation activities.

The geologic materials at a site represent a major controlling factor that determines the ultimate fate and transport of constituents in both the unsaturated and saturated zones. The most commonly employed site characterization technique typically involves intrusive drilling and sampling at a site to determine the spatial distribution of fuel hydrocarbons, based upon soil sample analyses. Continuous core sampling to completely characterize site lithology should be encouraged to improve understanding of migration pathways and barriers. In addition to analyzing soil samples over a vertical profile, it is important to conduct a soils analysis at lithologic interfaces and at zones of significant changes in soil moisture content.

Cone Penetrometry

The real-time availability of information is critical and part of an observational approach to site characterization, where a conceptual model of the site is continually reevaluated as data are iteratively gathered and interpreted. The refined conceptual model guides the placement of the next sampling location. The cone penetrometer system is especially attractive when the cost of quarterly monitoring groundwater wells is considered in assessing the cost of site characterization. The results of a cone penetrometer survey can be used to identify the optimum

location for final soil borings and groundwater monitoring wells for the purpose of long-term monitoring and remediation.

The typical cone penetrometer is mounted on a 20–60 ton truck and driven to the site requiring characterization. Cone penetrometer tools can collect both soil and groundwater samples as well as soil gas samples. A conical rod is hydraulically pushed into the ground. Some rigs are equipped with a hammer assist. The push rod tip can be equipped with a variety of sensors or soils and groundwater sampling tools. The cone penetrometer can characterize several important LUFT decision-making parameters, depending on the type sensor or tool used.

The probe can be used in either a “push” or “static” mode to gather a vertical profile at a single time, or left in place to gather data over an extended period of time. Sensors can provide electrical resistivity and pore pressure. Strain gauges measure the forces required to advance the rod tip, allowing indirect determination of the soil type. The data received is a continuous log of the geologic profile at a site and is superior to the current practice of sampling every 5 ft. Sampling every 5 ft often results in incomplete characterization of the hydrogeologic conditions at a site.

The cone penetrometer is limited by the presence of cobbles and boulders and generally cannot reach depths of greater than 100 ft below ground surface. Since a majority of California’s LUFT sites are located in regions with a minimum depth to groundwater of less than 50 ft, a cone penetrometer can easily gather information from five to 20 locations in a single day. The Department of Defense has made a major commitment to development of this technology, and the results of this effort can be leveraged for California’s benefit.

Laser Spectrometer System

One of the important sensor systems that has been developed for use with the cone penetrometer is a laser spectrometer that can identify a “fingerprint” of FHCs. The system takes advantage of the fact that certain substances fluoresce when a particular wavelength of light shines on them. The spectral emission as well as the fluorescent lifetime is unique to the substance. The fluorescent intensity indicates the concentration of the substance. As the penetrometer cone is advanced, a neodymium-yttrium aluminum garnet laser pumps light to a dye laser system to induce fluorescence of FHCs. Optical fibers are used to transmit the laser ultraviolet light through the penetrometer rod and a ruby window on the side of the cone. The resulting fluorescent emission light is returned thorough optical fibers to the surface for spectral analysis. The system can provide semi-qualitative and semi-quantitative data on the vertical spatial distribution of FHCs in minutes. The system, while in the demonstration phase, has been tested in the field and with detection limits as low as parts-per-million concentrations of total petroleum hydrocarbons in soils. This sensor system, used in conjunction with the cone penetrometer, holds promise as a relatively inexpensive means to provide needed information about FHC source masses. Concentration data can be provide from a relatively large number of sampling points, and source mass can be estimated with increased accuracy.

The use of laser-induced fluorescence with a cone penetrometer is also being tested by the U.S. Navy at the Port Hueneme, California, National Test Site for FHCs. This system is referred to as the Site Characterization and Analysis Penetrometer System (SCAPS). In addition, the SCAPS technology is one of the first being evaluated by the California Environmental Protection

Agency for certification. A variety of commercial manufacturers have embraced the technology and coupled it with advanced data visualization system to support informed, real-time field decision making.

Multi-analyte, Single-Fiber, Optical Sensors

Fiber-optic sensors offer tremendous potential for remote and *in situ* measurement of FHCs. Current methods for detecting FHCs require samples to be collected and submitted to laboratory analysis, which can take up to 30 days to get results. Optical sensors allow *in situ* measurement of FHCs in real time, saving both time and expense. A cone penetrometer fiber-optic probe has been developed that remains in place and provides continuous time sampling of groundwater or soil gas.

During the construction of a multi-analyte, single-fiber optical sensor, sensing regions are placed at precise locations at the end of single imaging optical fibers. The sensors are designed to fluoresce when illuminated by light at a particular excitation wavelength. Each individual sensor changes its fluorescence intensity according to changes in the concentration of a particular FHC chemical substance or pH. In addition, other compounds that can be measured include oxygen, carbon dioxide, and some inorganic ions.

Neutron Logging

Vadose zone characterization and monitoring can include the use of a neutron probe, used in concert with soil gas monitoring probes, to determine if unsaturated flow is taking place, assess the distribution of volatile constituents, and confirm the presence of conditions favorable for intrinsic bioremediation. Neutron probes can be successfully used in a variety of access tube construction configurations including stainless steel, carbon steel, PVC, and other casing materials. Use of the neutron probe to monitor the vadose zone can verify that FHCs are not subject to the driving force of recharging groundwater, especially at sites with effective asphalt or concrete subsurface barriers to infiltration. The neutron log can indicate strata where lithologic or high-moisture content barriers to vapor migration exist. Continuous cores taken at the time of access tube installation can indicate where soil gas monitoring points should be installed. The distribution of fine-grained sediments can be tracked with the neutron probe and as such, the layers in which soil gas, pore liquids, and free product presence are likely to be present can be tracked. At the early stages of a monitoring program, monthly or quarterly logging by neutron moderation can be effective in conducting an appraisal of the risk of recharging waters impacting underlying groundwater.

Electrical Resistance Tomography

Recently developed technologies have shown that images created by electrical resistivity may be successful in identifying the movement of vadose groundwater and spatial distribution of hydrocarbons in either the vadose or saturated zone. Electrical resistance tomography measurements made under simulated underground-tank test leaks were successful in simulating a leak and identifying the spread of contamination during an artificial release. These new,

developing geophysical technologies may be successful in developing 3-D images of the contaminant mass and migration rate.

Electrical resistance tomography creates an image of resistance to electrical current in the subsurface. To image the resistivity distribution between two boreholes, several electrodes are placed in each hole. The resistivity between all combinations of electrodes is measured and an image (tomograph) of the resistivity prepared. Since resistivity is sensitive to moisture content or the presence of FHCs in the subsurface, changes in resistivity can be used to image their spatial distribution in two dimensions, if two boreholes are used, or three dimensions if more than two boreholes are used.

Microcalorimetry To Monitor Bioremediation

Breakage and formation of chemical bonds generates heat, and the amount of heat, i.e., calories, released is measured in a calorimeter. A microcalorimeter is more sensitive than a standard calorimeter and can be used to detect correspondingly lesser amounts of heat released from small volumes and dilute samples of reactants. In living organisms, bond breaking and forming reactions are catalyzed by enzymes that are highly specific catalysts. Coupling the specificity of enzymes with the analytical sensitivity of a microcalorimeter provides a simple, fast, sensitive, and specific method for monitoring the bioremediation process. This technique can provide analysis of individual FHC components in complex mixtures, and the activity of FHC degrading bacteria.

References

- Ahmed, T. (1989), *Hydrocarbon Phase Behavior*. Vol. 7 in *Contributions in Petroleum Geology and Engineering*, Gulf Publishing Company, Houston, Texas.
- Anderson, M.P. (1984), "Movement of Contaminants in Groundwater: Groundwater Transport—Advection and Dispersion," in *Studies in Geophysics. Groundwater Contamination*, Panel on Groundwater Contamination, National Academy Press, Washington, D.C.
- Baedecker, M.J., L.M. Cozzarelli, J.R. Evans, and P.P. Hearn (1992), "Authigenic Mineral Formation in Aquifers Rich in Organic Material," in *Water-Rock Interaction*, Y.K. Kharaka and A.S. Maest (Eds.), A.A. Balkema, Rotterdam, Netherlands, 257.
- Baedecker, M.J., I.M. Cozzarelli, R.P. Eganhouse, D.I. Siegel, and P.C. Bennett (1993), "Crude Oil in a Shallow Sand and Gravel Aquifer—III. Biogeochemical Reactions and Mass Balance Modeling in Anoxic Groundwater," *Appl. Geochemistry* 8, 569.
- Barker, J.F., G.C. Patrick, and D. Major (1987), "Natural Attenuation of Aromatic Hydrocarbons in a Shallow Sand Aquifer," *Ground Water Monitoring Review* 7, 64.
- Bear, J., E. Nichols, J. Ziagos, and A. Kulshrestha (1994), *Effect of Contaminant Diffusion into and out of Low-Permeability Zones*, Lawrence Livermore National Laboratory, Livermore, California (UCRL-ID-115626).
- Becker, R.A., and J.M. Chambers (1984), *S, An Interactive Environment for Data Analysis and Graphics*, Wadsworth, Belmont, California.
- Becker, R.A., J.M. Chambers, and A.R. Wilks (1988), *The New S Language, A Programming Environment for Data Analysis and Graphics*, Wadsworth & Brooks, Pacific Grove, California.
- Beller, H.R., and M. Reinhard (1995), "The Role of Iron in Enhancing Anaerobic Toluene Degradation in Sulfate-Reducing Enrichment Cultures," *Microb. Ecol.* 30, 105.
- Bennett, P.C., D.E. Siegel, M.J. Baedecker, and M.F. Hult (1993), "Crude Oil in a Shallow Sand and Gravel Aquifer, 1, Hydrogeology and Inorganic Geochemistry," *Appl. Geochem.* 8, 529.
- Bishop, D.J., D.W. Rice, L.L. Rogers, and C.P. Webster-Scholten (1987), *Comparison of Field-Based Distribution Coefficients (K_d s) and Retardation Factors (R s) to Laboratory and Other Determinations of K_d s*, Lawrence Livermore National Laboratory, Livermore, California (UCRL-AR-105002).
- Borden, R.C., C.A. Gomez, and M.T. Becker (March–April 1995), "Geochemical Indicators of Intrinsic Bioremediation," *J. Ground Water* 33(2), 180.
- Bouwer, E.J., and P.L. McCarty (1984), "Modeling of Trace Organics Biotransformation in the Subsurface," *Ground Water* 22, 433.
- Buscheck, T.E., K.T. O'Reilly, and S.N. Nelson (1993), "Evaluation of Intrinsic Bioremediation at Field Sites," *Proc. Conf. Petroleum Hydrocarbons and Organic Chemicals in Ground Water*, November 10–12, Houston, Texas, 367.

- California Department of Water Resources (CDWR) (1975), *California's Ground Water, Bulletin No. 11*.
- Campbell, J.B. (1978), "Spatial Variation of Sand Content and pH within Single Contiguous Delineations of Two Soil Mapping Units," *Soil Sci. Soc. Amer. J.* **42**, 460.
- Chambers, J.M., and T.J. Hastie (1992), *Statistical Models in S*, Wadsworth & Brooks, Pacific Grove, California.
- Chambers, J.M., W.S. Cleveland, B. Kleiner, and P.A. Tukey (1983), *Graphical Methods for Data Analysis*, Wadsworth, Belmont, California.
- Chiang, C.Y., J.P. Salanitro, E.Y. Chai, J.D. Colthart, and C.L. Klein (Nov.-Dec. 1989), "Aerobic Biodegradation of Benzene, Toluene, and Xylene in a Sandy Aquifer—Data Analysis and Computer Modeling," *J. Ground Water* **27**(6), 823.
- Cole, G.M. (1994), *Assessment and Remediation of Petroleum Contaminated Sites*, Lewis Publishers, CRC Press, Boca Raton, Florida.
- Cozzarelli, I.M., and M.J. Baedecker (1992), "Oxidation of Hydrocarbons Coupled to Reduction of Inorganic Species in Groundwater," *Water-Rock Interaction, Vol. 1: Low Temperature Environments*, Y.K. Kharaka and A.S. Maest (Eds.), A.A. Balkema, Brookfield, Massachusetts, 275.
- Cozzarelli, I.M., R.P. Eganhouse, and M.J. Baedecker (1990), "Transformation of Monoaromatic Hydrocarbons to Organic Acids in Anoxic Ground Water Environment," *Environmental Geology and Water Science* **16**, 135.
- Cozzarelli, I.M., M.J. Baedecker, R.P. Eganhouse, and D.F. Goerlitz (1994), "The Geochemical Evolution of Low-Molecular-Weight Organic Acids Derived from the Degradation of Petroleum Contaminants in Groundwater," *Geochim. Cosmochim. Acta* **58**, 863.
- Domenico, P.A., and G.A. Robbins (1985), "A New Method of Contaminant Plume Analysis," *Groundwater* **23**(4), 476.
- Draper, N.R., and H. Smith (1981), *Applied Regression Analysis* (2nd Ed.), John Wiley & Sons, New York, New York.
- Eganhouse, R.P., M.J. Baedecker, I.M. Cozzarelli, G.R. Aiken, K.A. Thorn, and T.F. Dorsey (1993), "Crude Oil in a Shallow Sand and Gravel Aquifer, 2, Organic Geochemistry," *Appl. Geochem.* **8**, 551.
- Falta, R.W., I. Javandel, K. Pruess, and P. Witherspoon (1989), "Density Driven Flow of Gas in the Unsaturated Zone Due to the Evaporation of Volatile Organic Compounds," *Water Resources Research* **25**(10), 2159.
- Finley, B., D. Proctor, P. Scott, N. Harrington, D. Paustenbach, and P. Price (1994), "Recommended Distributions for Exposure Factors Frequently Used in Health Risk Assessment," *Risk Analysis* **14**(4), 533.
- Freeze, R.A., and J.A. Cherry (1979), *Groundwater*, Prentice-Hall, Englewood Cliffs, New Jersey.

- Haag, F., M. Reinhard, and P.L. McCarty (1991), "Degradation of Toluene and *p*-Xylene in Anaerobic Microcosms: Evidence for Sulfate as a Terminal Electron Acceptor," *Environmental Toxicology and Chemistry* 10, 1379.
- Hunt, J.R., N. Sitar, and K.S. Udell (1988), "Nonaqueous Phase Liquid Transport and Cleanup. 1. Analysis of Mechanisms," *Water Resources Research* 24:8, 1247.
- Isaaks, E.H., and R.M. Srivastava (1989), *An Introduction to Applied Geostatistics*, Oxford University Press, New York, New York.
- Johnson, P.C., and R.A. Ettinger (1991), *Environmental Science Technology*, 25(8), 1445-1452.
- Jury, W.A., W.F. Spencer, and W.J. Farmer (1983), *J. Environmental Quality*, 12, 558-564.
- Jury, W.A., D. Russo, G. Streile, and H. El Abd (1990), "Evaluation of Volatilization by Organic Chemicals Residing below the Soil Surface," *Water Resources Research* 26(1), 13.
- Karickhoff, S.W., D.S. Brown, and T.A. Scott (1979), "Sorption of Hydrophobic Pollutants on Natural Sediments," *Water Research* 13, 241.
- Layton, D.W. (1993), "Metabolically Consistent Breathing Rates for Use in Dose Assessments," *Health Physics* 64(1), 23.
- Layton, D.W., L.R. Anspaugh, K.T. Bogen, and T. Straume (1993), *Risk Assessment of Soil-Based Exposures to Plutonium at Experimental Sites Located on the Nevada Test Site and Adjoining Areas*, Lawrence Livermore National Laboratory, Livermore, California (UCRL-ID-112605).
- McAllister, P.M., and C.Y. Chiang (Spring 1994), "A Practical Approach To Evaluating Natural Attenuation of Contaminants in Ground Water," *Ground Water Monitoring and Remediation*.
- McCullagh, P., and J.A. Nelder (1989), *Generalized Linear Models*, 2nd ed., Chapman and Hall, London, England.
- McNab, W.W., Jr., and T.N. Narasimhan (1995), "Reactive Transport of Petroleum Hydrocarbon Constituents in a Shallow Aquifer: Modeling Geochemical Interactions Between Organic and Inorganic Species," *Water Resources Research* 31(8), 2027.
- Meriam, J.L. (1975), *Dynamics*, John Wiley & Sons, New York, New York.
- National Research Council (1994), *Alternatives for Ground Water Cleanup*, National Academy Press, Washington, D.C.
- Press, W.H., S.A. Teukolsky, W.T. Vetterling, and B.P. Flannery (1992), *Numerical Recipes* (2nd Ed.), Cambridge University Press, New York, New York.
- Reinhard, M. (1993), "In-Situ Bioremediation Technologies for Petroleum-Derived Hydrocarbons Based on Alternate Electron Acceptors (Other than Molecular Oxygen)," *Handbook of Bioremediation*, Lewis Publishers, Ann Arbor, Michigan, 131.
- Rifai, H.S., P.B. Bedient, J.T. Wilson, K.M. Miller, and J.M. Armstrong (1988), "Biodegradation Modeling at an Aviation Fuel Spill Site," *J. Environmental Engineering, ASCE* 114, 1007.
- Salanitro, J.P. (Fall 1993), "The Role of Bioattenuation in the Management of Aromatic Hydrocarbon Plumes in Aquifers," *Ground Water Monitoring and Remediation*, 150.

- Salanitro, J.P., L.A. Diaz, M.P. Williams, and H.L. Wisniewski (1993), "Simple Method To Estimate Aromatic Hydrocarbon Degrading Units (Microbes) in Soil and Ground Water," Presented at the 1993 Int. Symposium on Subsurface Microbiology (ISSM93), September 19-24, Bath, England.
- Schwalen, E.T., K.L. Kiefer, D.P.H. Hsieh, and T.E. McKone (April 1995), "The Distribution of Landscape Variables in CalTOX within California," Draft Report, University of California, Davis, Department of Environmental Toxicology, Department of Toxic Substances Control (DTSC), Davis, California.
- Seber, G.A.F., and C.J. Wild (1989), *Nonlinear Regression*, John Wiley & Sons, New York, New York.
- Silka, L.R. (1986), "Simulation of the Movement of Volatile Organic Vapor Through the Unsaturated Zone as It Pertains to Soil-Gas Surveys," *Proc. Petroleum Hydrocarbons and Organic Chemicals in Ground Water Conf. and Exposition*, Houston, Texas (November 13-15, 1985), American Petroleum Institute and National Water Well Association.
- Thomas, H.E., and D.A. Phoenix (1976), *Summary Appraisals of the Nation's Ground Water Resources—California Region*, U.S. Geological Survey, Menlo Park, California, USGS Paper 813-E.
- U.S. Environmental Protection Agency (EPA) (1990), *Risk Assessment, Management and Communication of Drinking Water Contamination*, U.S. Environmental Protection Agency, Office of Drinking Water, Office of Water (Washington, D.C.); Office of Technology Transfer and Regulatory Support, and Office of Research and Development (Cincinnati, Ohio), EPA/625/489/024.
- Vogel, T.M., C.S. Criddle, and P.L. McCarty (1987), "Transformations of Halogenated Aliphatic Compounds," *Environ. Sci. Technol.* **21**, 722.
- Wilson, J.T., F.M. Pfeffer, J.W. Weaver, D.H. Kampbell, R.S. Kerr, T.H. Wiedemeier, J.E. Hansen, and R.N. Miller (1994), "Intrinsic Bioremediation of JP-4 Jet Fuel," *Proc. Symposium on Intrinsic Bioremediation of Groundwater*, Denver, Colorado (August 30-September 1), 60.

Acronyms

ASTM	American Society for Testing and Materials
BTEX	benzene, toluene, ethylbenzene, total xylenes
FHC	fuel hydrocarbon
LUFT	leaking underground fuel tank
PDF	probability distribution function
ppb	parts per billion
RBCA	risk-based corrective action
SCAPS	Site Characterization and Analysis Penetrometer System
SWRCB	State Water Resources Control Board
SF RWQCB	San Francisco Regional Water Quality Control Board
TASL	target action screening level
TPHg	total petroleum hydrocarbon-gasoline
UC	University of California
UST	underground storage tank
2-D	two-dimensional
3-D	three-dimensional

